



NOVA Sub-mm  
Instrumentation  
Group

## Improving Band 9 Sensitivity by Advanced Tuning Algorithms — Final Study Report

FEND-40.02.09.00-1944-C

Version: C

Status: Released

2020-01-07

Prepared by:		
Name(s) and Signature(s)	Organisation	Date
Ronald Hesper Jan Barkhof Tobias Vos	RuG/NOVA	2020-01-07
Approved by:		
Name(s) and Signature(s)	Organisation	Date
Pavel Yagoubov	ESO	2019-12-23
Released by:		
Name(s) and Signature(s)	Organisation	Date
Ronald Hesper	RuG/NOVA	2020-01-10

 <p>NOVA Sub-mm Instrumentation Group</p>	<p><b>Improving Band 9 Sensitivity by Advanced Tuning Algorithms — Final Study Report</b></p>	<p>DocID: FEND-40.02.09.00-1944-C Version: C Date: 2020-01-07 Status: Released Page: 2 of 44</p>
------------------------------------------------------------------------------------------------------------------------------------	-----------------------------------------------------------------------------------------------------------	------------------------------------------------------------------------------------------------------------------

## Revision history

Version	Date	Affected section(s)	Change request #	Reason/Initiation/Remarks
A	2019-12-02	All	N/A	Initial document, based on NOVA-ATA-0002-B “Advanced Tuning Midterm Review Report”, 2019-04-04
B	2019-12-20	1.2.3, 3.1, 4, 5, 6 (new section)	RIDs	Updates after final review (2019-12-13); other minor improvements and additions.
C	2020-01-07	4.9	Review	Function to find <i>N</i> th minimum mentioned. Figure 23 reformatted. Removal of change marks. Minor typographical and layout corrections.

	<b>Improving Band 9 Sensitivity by Advanced Tuning Algorithms — Final Study Report</b>	DocID: FEND-40.02.09.00-1944-C Version: C Date: 2020-01-07 Status: Released Page: 3 of 44
-----------------------------------------------------------------------------------	----------------------------------------------------------------------------------------------------	-------------------------------------------------------------------------------------------------------

## Contents

<b>1</b>	<b>Introduction</b>	<b>4</b>
1.1	Scientific driver . . . . .	4
1.2	Technical description . . . . .	4
1.2.1	Introduction . . . . .	4
1.2.2	The search among remaining Band 9 junctions . . . . .	5
1.2.3	The problem of automatic tuning . . . . .	7
1.3	Goals of the Study . . . . .	10
<b>2</b>	<b>Software infrastructure</b>	<b>11</b>
2.1	Design principles . . . . .	11
2.2	Code structure . . . . .	12
2.3	Usage (as compared to <i>Rodrigo</i> ) . . . . .	15
2.3.1	Measurement scripts . . . . .	15
2.3.2	Data files . . . . .	17
2.3.3	Operation points files . . . . .	17
<b>3</b>	<b>The old algorithms</b>	<b>18</b>
3.1	Magnet current . . . . .	18
3.2	Bias voltage and LO power (operation points) . . . . .	21
3.3	Mixer qualification . . . . .	24
<b>4</b>	<b>Automating the tuning algorithm</b>	<b>25</b>
4.1	Demag-deflux cycle . . . . .	25
4.2	Determining the gap current . . . . .	25
4.3	Determining the critical current . . . . .	26
4.4	Obtaining the initial suppression point . . . . .	27
4.5	Refining the suppression . . . . .	27
4.6	Verifying the suppression . . . . .	27
4.7	The final tuning algorithm . . . . .	28
4.8	Application of the algorithm . . . . .	29
4.9	Selecting an arbitrary minimum . . . . .	30
<b>5</b>	<b>Improvement of existing ALMA mixers</b>	<b>32</b>
5.1	Analysis of historical ALMA data . . . . .	32
5.2	Analysis of historical CHAMP+ data . . . . .	33
5.3	Magnetic field dependence of the noise temperature . . . . .	34
5.4	Synthesis — prospect of improved ALMA Band 9 performance . . . . .	37
5.5	Influence of suppression on other performance parameters . . . . .	38
5.5.1	Stability . . . . .	38
5.5.2	Gain compression . . . . .	39
5.5.3	Frequency dependence of the Josephson minima . . . . .	40
<b>6</b>	<b>Conclusion and outlook</b>	<b>42</b>
6.1	Conclusions . . . . .	42
6.2	Outlook . . . . .	42
<b>7</b>	<b>References</b>	<b>44</b>

	<b>Improving Band 9 Sensitivity by Advanced Tuning Algorithms — Final Study Report</b>	DocID: FEND-40.02.09.00-1944-C Version: C Date: 2020-01-07 Status: Released Page: 4 of 44
-----------------------------------------------------------------------------------	----------------------------------------------------------------------------------------------------	-------------------------------------------------------------------------------------------------------

# 1 Introduction

In this section we formulate the problems and the goals of the study. Most of this material is derived from the original study proposal [1]. It is included here for easy reference.

## 1.1 Scientific driver

The scientific driver for the proposed study is an improvement of the sensitivity of the existing ALMA Band 9 receivers that have been delivered by the NOVA Submillimeter Instrumentation Group to the observatory, without any hardware intervention. This ties in with the Recommended Development Path number 2 (“Larger bandwidths and better receiver sensitivity”) in the ASAC recommendations for ALMA 2030 [2]. It also corresponds to Pathway No. 05 (“Sensitivity: Lower noise Rx”) in the ALMA Development Working Group Report “Pathways to Developing ALMA” [3].

We expected, and the results of the study confirm this, that the noise temperature of the majority of the delivered mixers can be improved by about 10 K, and some as much as 20 K, by developing advanced tuning algorithms. Since the typical double sideband (DSB) noise temperature of the mixers is of the order of 100 K, this means an increase of about 10% (and possibly more) in sensitivity for the entire array “for free”. The investment to be made for this is the current study and the effort of implementing it in the ALMA front end software.

Of course, any insights gained in this study can also be used in other instruments that use the ALMA Band 9 mixers (CHAMP+, SEPIA, LLAMA), and, with proper modifications, likely with other SIS-based bands as well.

## 1.2 Technical description

### 1.2.1 Introduction

The SIS mixer devices that are employed in the ALMA Band 9 receiver cartridges [4] need a magnetic field to suppress the Josephson effect, as Josephson current flowing through the junction leads to excess noise and hence reduced sensitivity. Contrary to lower-frequency bands, where a simple setpoint for the magnet current or even permanent magnets are successfully employed, Band 9 mixers require an accurate tuning of the field (generated in a superconducting coil close to the junction) for optimal performance.

In an ideal rectangular junction with the magnetic field parallel to one of the axes, the Josephson current as function of field theoretically shows a  $|\sin(x)/x|$  behaviour (fig. 1). In a circular junction, on the other hand, the current follows a  $|J_1(x)|$  function, with  $J_1(x)$  a Bessel function of the first kind. In practice, with slightly rounded square junctions, and the presence of interactions between the field and surrounding superconduction films, these functions are modified. Typically, they still show a more or less equidistant sequence of minima, but the particular shape of them will be different.

In principle, good Josephson suppression can be obtained in any of those minima. Due to geometrical effects and the above-mentioned interactions with the films, however, some of the minima may be sharp, while others are relatively shallow. When this is the case, for stability

	<b>Improving Band 9 Sensitivity by Advanced Tuning Algorithms — Final Study Report</b>	DocID: FEND-40.02.09.00-1944-C Version: C Date: 2020-01-07 Status: Released Page: 5 of 44
-----------------------------------------------------------------------------------	----------------------------------------------------------------------------------------------------	-------------------------------------------------------------------------------------------------------

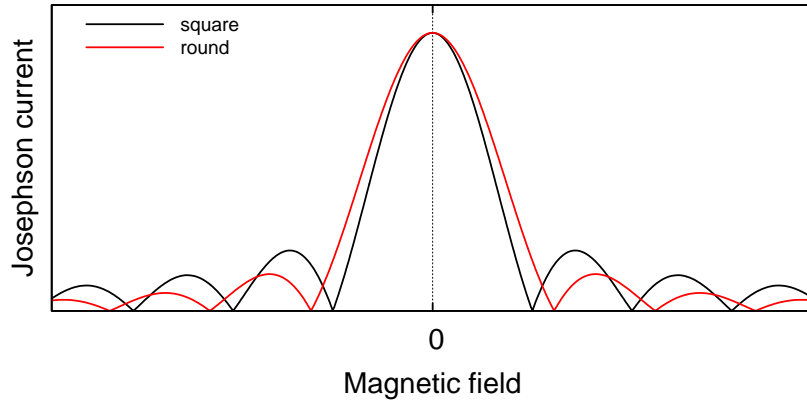


Figure 1: Theoretical behaviour of the Josephson current in square (black,  $\propto |\sin(x)/x|$ ) and round (red,  $\propto |J_1(x)/x|$ ) SIS junctions as function of magnetic field applied in-plane with respect to the junction.

reasons often a shallower minimum is chosen, to be less sensitive to small variations in the magnetic field due to stray fields or noise in the bias circuits, as well as to variations between bias units. On the other hand, the noise temperature of the mixer tends to increase with magnetic field due to the overall suppression of the superconducting state. These two effects together will determine the choice of minimum to use.

In real-life junctions, the dependence typically is even less ideal. Magnetic flux, trapped locally in the superconducting films, tends to distort the picture, as do inhomogeneities in the films. Especially in the wide-band AlN-barrier junctions that were employed in most production Band 9 cartridges, often step-like and hysteretic effects are seen. Additionally, even in cases where the critical current seems to be suppressed well, the Josephson features in the IF power vs. bias voltage plots were not always acceptably small. Apart from out-of-spec noise temperature, unfavourable suppression curves were the main reason for rejection of mixers during production.

In the mixer design actually used in Band 9, only the first minimum is reasonably sharp; the second and subsequent ones are much more shallow. Because of considerations of tuning stability and reproducibility, we almost always chose to use the second minimum. At this value of the magnetic field, we could find a sufficient number of junctions with a noise temperature well within the ALMA specification. Although this was no specification from the project, we made the presence of a usable second minimum one of our internal acceptance criteria of the mixers, to ensure good tunability during operation.

### 1.2.2 The search among remaining Band 9 junctions

Despite the arguments given in the previous section about the preferred suppression in the second minimum, it is also an area of potential improvement. During a recent re-testing campaign of left over Band 9 junctions for use in other projects, we noticed that a significant fraction of them could successfully be operated in the first minimum, often with a pronounced improvement in noise temperature.

Examples for two mixer devices are shown in figure 2. These two devices show an improvement of the order of 10 K in noise temperature each time the suppression is lowered one step (from

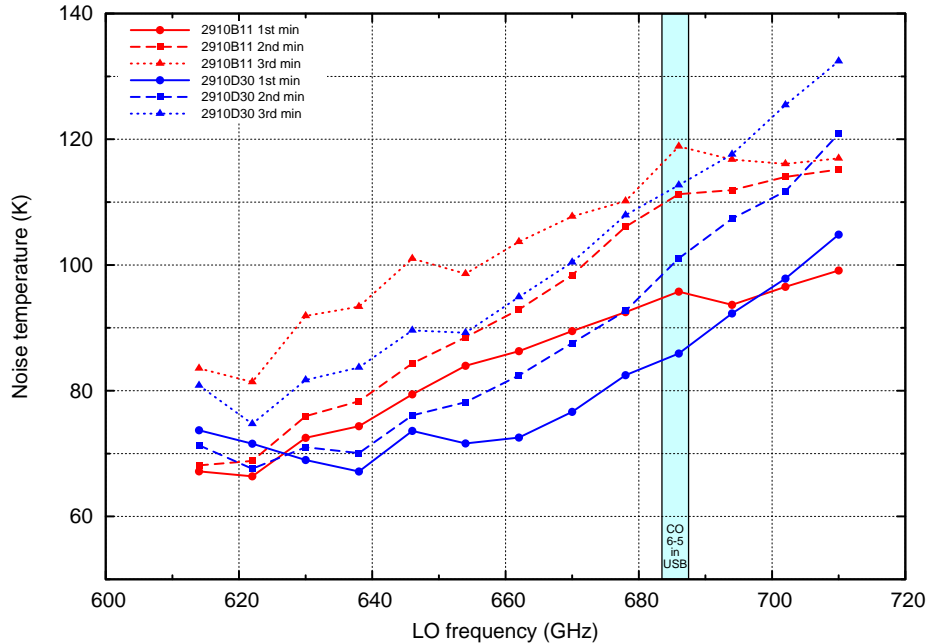


Figure 2: Double-sideband noise temperature of two Band 9 mixers, Josephson-suppressed in subsequent minima of the critical current vs. magnet current function. The shaded area indicates the frequencies for which the (non-redshifted) CO(6–5) line at 691 GHz is in the upper sideband.

third to second to first minimum). Table 1 shows an overview of several more mixers which have recently been remeasured in subsequent minima. Each line in this table represents a measurement in the same system (cartridge number, LO, bias box, etc.), so good comparisons between the minima can be made. A lot of historical data from the Band 9 production campaign are available as well, but since these were taken in different systems (especially the LO seems to have a relatively large influence), comparison between them is less straightforward.

The table gives the minimum, maximum and averaged noise temperatures over the band, and the noise temperature at 686 GHz (LO), which has the important CO(6–5) line at 691 GHz in the upper sideband. Although there is quite a bit of variation in improvement between the

SIS	First min					Second min					Third min				
	$I_m$	$T_{min}$	$T_{CO}$	$T_{max}$	$T_{avg}$	$I_m$	$T_{min}$	$T_{CO}$	$T_{max}$	$T_{avg}$	$I_m$	$T_{min}$	$T_{CO}$	$T_{max}$	$T_{avg}$
2803B48	6.9	70	97	98	85	12.9	73	109	115	93					
2803D72						10.2	67	91	104	80	19.7	89	134	137	114
2906A37	6.0	75	108	121	95	9.1	77	110	116	96					
2910B11	7.8	70	101	104	89	11.7	72	117	121	98	16.1	85	125	125	108
2910D30	10.3	71	90	110	84	13.7	71	106	127	92	17.6	78	118	139	104
2910D54	5.5	83	107	119	97	9.2	84	118	132	104					
2910D60	6.1	74	95	111	88	10.8	77	103	120	93					

Table 1: Noise temperatures for a small selection of left-over Band 9 mixers that were retested recently, suppressed in different minima. SIS: junction identifier,  $I_m$ : magnet current (mA).  $T_{min}$ : minimum,  $T_{max}$ : maximum,  $T_{avg}$ : average noise temperature.  $T_{CO}$ : noise temperature at CO 6–5 frequency. Some identifications of the order of minima are tentative.

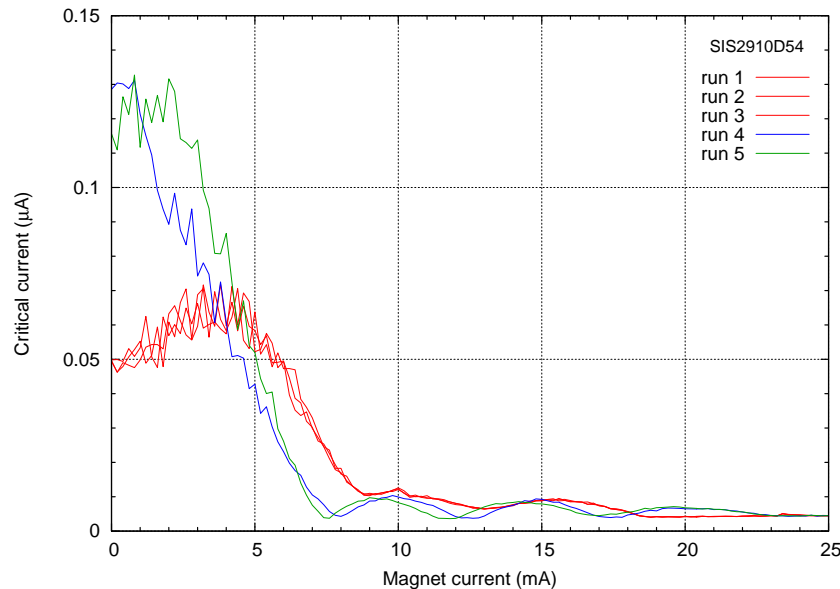


Figure 3: Example of the critical (Josephson) current as function of magnet current for a Band 9 AlN-barrier mixer. The different traces are taken after subsequent demag-deflux cycles, which clearly can result in slightly different behaviour each time — or a complete miss. This particular junction is also listed in Table 1, but the exact current values of the minima are slightly different due to being measured in different mixerholders, with different coils and magnetic coupling coefficients.

mixers, numbers of around 10 K when going from second to first minimum seem rather typical.

It should be noted that these mixers are left-overs from the Band 9 production campaign, and as such not fully representative for the operational ones. On one hand, the delivered mixers were almost never tested in the first minimum, so we do not have a clear idea how many of them could be used there. On the other hand, they were selected for “tunability”, so they may be more likely to have usable first minima than the left-over ones.

### 1.2.3 The problem of automatic tuning

As mentioned above, real-life junctions (especially the wide-band AlN-barrier junctions) often exhibit non-ideal behaviour in their critical-current vs. magnetic field dependence. Figures 3 and 4 show some common examples of this.

In both cases, the critical current curve was recorded several times, each time after demagnetizing the core and defluxing the mixer. A deflux cycle consists of a pulse on a small heater built into the mixer backpiece to drive it momentarily out of superconductivity, in order to let trapped flux lines escape the superconducting films. Because any remanent field in the magnetic core would immediately freeze in when superconductivity returns, each deflux pulse is preceded by a degaussing (demagnetizing) cycle of the magnet system. Together we call this a demag-deflux cycle. Since the absence of remanent field is essential during the defluxing, and we have no independent way to determine its presence, we always combine these cycles.

Figure 3 belongs to a mixer that shows several different suppression curves after each demag-

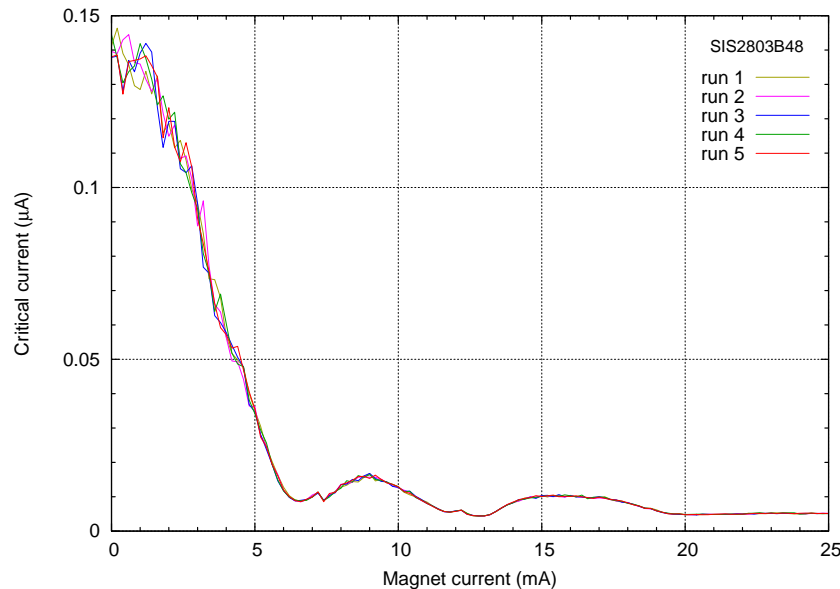


Figure 4: Another example of the Josephson current as function of magnet current for a Band 9 AlN-barrier mixer, after subsequent deflux cycles. The traces in this case reproduce, but there are clear jumps close to both first and second minimum. This mixer was rejected for that reason for ALMA production.

deflux cycle. The blue and green ones (4 and 5) both look pretty healthy, but are nevertheless different. In the second minimum (around 12 mA), both probably will give good suppression. In the first minimum, however, due to its sharper character, a common suppression point is not achievable. The red curves (1–3) look totally different from the others, although the performance in one of their minima may still be acceptable. The fact that these reproduce several times points to some defect in the films close to the junction that is prone to retain a flux line. This figure is an extreme example; most delivered junctions show more consistent curves. On the other hand, many junctions would display deviating behaviour every so often after a deflux cycle. In order to be able to deliver a sufficient number of mixers in the given time frame while maintaining good operability, we used a criterion of a minimum number of consecutive demag-deflux cycles that should give identical suppression curves for the mixer to be accepted. Nevertheless, there is no hard guarantee that all mixers will end up in the same regime every time. Any stable automatic suppression algorithm therefore must be able to judge whether a demag-deflux cycle was successful. In order to make the first minimum usable in a reliable way, this should happen at a quite detailed level.

Another issue is demonstrated in fig. 4. Here, the curves reproduce very well over five cycles, but sharp steps are observable close to the first and second minima. The cause of these steps is not completely understood, but they are quite common in the AlN-barrier junctions (as opposed to the AlO<sub>x</sub> junctions in which they were rarely observed). The traces shown in this figure were all recorded going up in current, but often clear hysteresis can be seen around these steps when going back and forth. A step close to the second minimum, as this particular junction shows, was only a criterion for rejection if it indeed showed out-of-spec stability (or other performance parameters). Junctions were never rejected because of steps close to the first minimum, since this was not intended to be used in operation. This means that either an investigation should be made on the number of junctions that have clean first minima, or that the tuning algorithm is robust against the presence of such steps. The former can probably be

	<b>Improving Band 9 Sensitivity by Advanced Tuning Algorithms — Final Study Report</b>	DocID: FEND-40.02.09.00-1944-C Version: C Date: 2020-01-07 Status: Released Page: 9 of 44
-----------------------------------------------------------------------------------	----------------------------------------------------------------------------------------------------	-------------------------------------------------------------------------------------------------------

executed for a large extent with the mixer test results that are in our data archive. Another thing that should be investigated is how harmful the close presence of a step is, *i.e.*, to answer the question whether a junction like the one in fig.4 would still be usable and stable in the first minimum (at 6.5 mA, say).

The illustrations shown above are of the critical current vs. magnetic field behaviour because it supplies the easiest insight in the problem. In practice, however, the best suppression is found by looking at the relation of IF-power vs. magnetic field. This is much more sensitive, and has a more direct relationship with the noise temperature. It is also more complicated, however, since it depends strongly on the mixer bias voltage and LO frequency (contrary to the critical current plots, which are frequency-independent to a large degree). Figure 5 shows an example of a reasonably well-behaved junction. It is likely that a sensitive and stable algorithm may use the critical current to find candidate suppression points, but that access to the IF power is necessary for refinement and for assuring that a good bias point can be found.

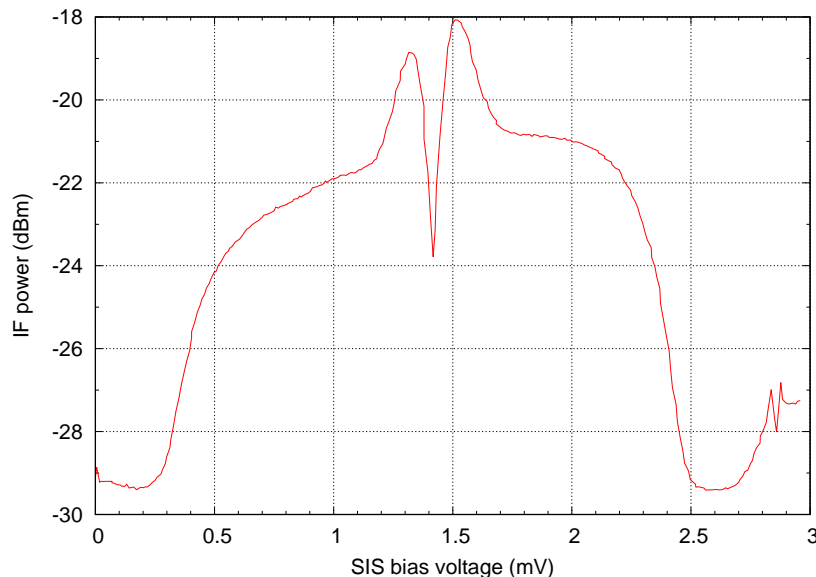


Figure 5: Typical IF power vs. SIS bias voltage curve for a reasonably well-behaved junction, suppressed at the second minimum. The double peak structure near the centre is due to the remaining Josephson current, although the critical current has been suppressed effectively. The amplitude of the Josephson feature is rather large (about 6 dB), but still a sufficiently large and stable area right of it (say, 1.8–2 mV) is available for biasing.

Up to recently, the judgement of the suitability of a mixer, and the correctness of both the suppression and the chosen bias voltage was mainly done by eye. Our overall goal is to automate these tuning procedures in a way that they can be performed, more or less on the fly, at the observatory, in order to achieve reliable tuning in points that are more critical than used traditionally, but with a promise of enhanced performance.

The discussion up to now was mainly focussed on the AlN junctions, as these form the majority of installed junctions (116 AlN vs. 30 AlO<sub>x</sub>) and are the most challenging to tune. The AlO<sub>x</sub> junctions do not generally show the multi-mode or hysteretic behaviour seen in the AlN ones. Nevertheless, although we expect that any algorithm capable of successfully tuning the former will have no problem tuning the latter, we tested this experimentally as reported in section 4.8.

 <p>NOVA Sub-mm Instrumentation Group</p>	<p><b>Improving Band 9 Sensitivity by Advanced Tuning Algorithms — Final Study Report</b></p>	<p>DocID: FEND-40.02.09.00-1944-C Version: C Date: 2020-01-07 Status: Released Page: 10 of 44</p>
------------------------------------------------------------------------------------------------------------------------------------	-----------------------------------------------------------------------------------------------------------	-------------------------------------------------------------------------------------------------------------------

### 1.3 Goals of the Study

The goals of the project are to

- study the possibility of automatically tuning the Josephson suppression field in order to reliably end up in the first (or any other desired) minimum;
- study the possibility of automatically determining the success or failure of a demag-deflux cycle; and
- estimate the number of operational mixers that could be improved this way (and by how much) based on existing NOVA test data.

 <p>NOVA Sub-mm Instrumentation Group</p>	<p><b>Improving Band 9 Sensitivity by Advanced Tuning Algorithms — Final Study Report</b></p>	<p>DocID: FEND-40.02.09.00-1944-C Version: C Date: 2020-01-07 Status: Released Page: 11 of 44</p>
------------------------------------------------------------------------------------------------------------------------------------	-----------------------------------------------------------------------------------------------------------	-------------------------------------------------------------------------------------------------------------------

## 2 Software infrastructure

Note: this chapter is unchanged with respect to the Midterm Review Report[5].

At the beginning of the Band 9 production period, the control of the cartridge measurement setup was automated to a large extent. For this, a dedicated scripting system was constructed, informally called *Rodrigo*, after the original author Rodrigo Rivas, with a simple but *ad-hoc* language syntax. While this system performed to full satisfaction for routine and standardized test procedures during the Band 9 production, and after some modifications, even for the later Band 5 production, it was clearly not up to the job of carrying out sophisticated algorithms. The main features missing are conditional statements, loops and structured data storage. Instead of extending the language with these kind of constructs, we chose to reimplement the entire measurement system in a readily available and widely-used open-source interpreted language, Python. This immediately gives us the full power of a modern and proven programming environment without trying to reinvent the wheel.

In the rest of this section the transition from the traditional *Rodrigo* system to the new system, for the moment called *Novasoft*, will be described. A reasonable acquaintance with the Python language is assumed here. This section is a condensed version of the internship report of Tobias Vos, which is available in full in the Appendix of the Midterm Review Report[5, 6, 7].

### 2.1 Design principles

A complete rewrite of *Rodrigo* into Python does not merely entail a port to a different programming language. In fact, it provides an excellent opportunity for a full system redesign, with a chance to replace the bad parts while keeping the good. To pinpoint both of these, users of the system were consulted and in addition, the *Rodrigo* code was extensively re-examined. The findings were as follows:

Pros of traditional *Rodrigo*:

- It does the job for production qualification;
- The instrument configuration file approach is very clear and dynamic;
- Logging all commands and replies both to the GUI and to a log file is highly convenient and allows *a posteriori* review of measurement conditions;
- Saving raw data to `.txt` files allows us to process it whenever and however we want to;
- Early error detection: error checking is extensive and communicated well to the user;
- The GUI is convenient and only starts interacting with the receiver when it is asked to;
- Values that should only be changed in small increments have a built-in protection mechanism limiting the rate of change.

Cons:

- The parsing process puts limitations on measurement scripts (*e.g.*, no conditional statements or loops);
- Extending it, *e.g.*, adding a new type of instrument or measurement, requires adding code in many different places;
- The code is inextricably intertwined with the GUI, to the point that there is no other way to interact with the software;

 <p>NOVA Sub-mm Instrumentation Group</p>	<p><b>Improving Band 9 Sensitivity by Advanced Tuning Algorithms — Final Study Report</b></p>	<p>DocID: FEND-40.02.09.00-1944-C Version: C Date: 2020-01-07 Status: Released Page: 12 of 44</p>
------------------------------------------------------------------------------------------------------------------------------------	-----------------------------------------------------------------------------------------------------------	-------------------------------------------------------------------------------------------------------------------

- The code relies heavily on closed-source National Instruments' LabWindows/CVI software, with associated costs in the order of a thousand Euros per year for licensing, and it only works under Microsoft Windows;
- An instrument configuration file can only be loaded when all devices (or at least their interface boards) are physically present, meaning that we might need different `.cfg` files for slight variations of the same experimental setup. This could also be considered as an advantage, because the user will immediately be notified of any missing instruments. Therefore, both options should be supported;
- It only allows us to use one CAN-bus port (the main communication channel to the cartridge bias electronics) at a time;
- There is a severe lack of documentation.

To summarize, apart from getting rid of the ad-hoc interpreter, *Novasoft* should be designed in such a way that it can easily be understood, used and extended. If done in a sufficiently generalized way, this will not just be useful for testing or controlling ALMA receivers, but for any instrumental setup used by NOVA internally or by fellow instrumentation groups. Apart from retaining all features that made *Rodrigo* an effective tool, these are the two guiding principles that underlie the new design. In the process, the aim is to maintain some level of backward compatibility and operator familiarity with *Rodrigo*.

## 2.2 Code structure

Getting rid of the existing script interpreter has its consequences for the structure of the *Novasoft* code. Rather than the software reading a “custom” script, it is now the Python script itself importing the software. Furthermore, we have tried to make it more widely applicable in a number of ways:

- We have opted for an object-oriented design. Each instrument is now represented by an object of some instrument class. Each instrument class inherits from an abstract base class `InstrumentBase`, which defines a common interface for all instrument types. As a result, one can simply define a new type, while the rest of the code stays the same.
- The loading and saving of instrument configuration files was revised. Thanks in part to the use of regular expressions, these functions now automatically work for any regular instrument type. The software’s documentation explains how to handle composite instrument types. The difference between the two is explained below.
- The software was made more configurable. For example, one can now easily define a new format for saving data (`storage.py`), or change the default save format, log file, etc., without diving into the source code (`config.py`).
- The *Novasoft* library supports both Python 2.7 and 3.4+.

Figure 6 shows the overall structure of the *Novasoft* system. Compared to its predecessor, it has a clearer structure and more extensive documentation.

The purpose of the various modules is as follows:

- **`instruments`** is a subpackage that handles all hardware interaction. It is described in more detail below.
- **`config.py`** implements a package-wide settings facility. It defines a dictionary named `_defaults` and a dictionary-like class `_RcParams`. It initializes and exports `config` as the singleton `_RcParams(_defaults)`. A user can modify settings at runtime in several ways:

	<b>Improving Band 9 Sensitivity by Advanced Tuning Algorithms — Final Study Report</b>	DocID: FEND-40.02.09.00-1944-C Version: C Date: 2020-01-07 Status: Released Page: 13 of 44

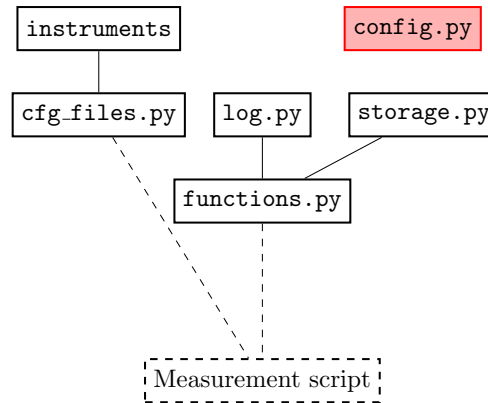


Figure 6: Top-level structure of the *Novasoft* system

```

1 from novasoft.config import config
2 config['FANCY_CFG'] = False
3 config.rc('WAIT_CAN'=0.2, 'RETRY_N_CAN'=5)
4 config.rcdefaults() # Restore default settings (run commands)

```

For example, 'FANCY\_CFG' is a boolean that determines whether instrument configurations are saved in a way that represents the code or in a way that pleases the eye. 'WAIT\_CAN' and 'RETRY\_N\_CAN' were also present in *Rodrigo*. The reader is referred to the source code for a full list.

- **cfg\_files.py** handles reading and writing to instrument configuration files. Its main functions are `load_cfg`, which turns a `.cfg` file into a dictionary of instruments, and `save_cfg`, which does the opposite. Both use a number of helper functions. This module also specifies how certain attribute-value pairs should be formatted. For example, 'min\_val' maps to 'Minimum value' (if 'FANCY\_CFG'), whereas CAN addresses are displayed as hexadecimal values. `ns.config['SAVE_DEFAULTS']` determines whether default values are saved. If set to `False`, `save_cfg` omits instrument attributes that equal their default value.
- **log.py** provides *Novasoft* with event logging capabilities. It implements a function `log` and a function decorator `log_cmd`. The former logs a timestamped message to a log file (default: `ns.config['LOG_FILENAME']`) and/or to the terminal (depending on the value of `ns.config['LOG_TERMINAL']`). `log_cmd` decorates most functions defined in `functions.py`, meaning that they are automatically logged when called.
- **storage.py** is used for saving measurement data in one of several formats. It defines a dictionary `_formats`, which maps each format to a certain save function and to one or more filename extensions. For example, ASCII is mapped to `_save_ASCII`, which is implemented further down the module, and to the `.txt` and `.dat` filename extensions. The user only has to worry about `save_data`, which accepts a format argument. If `None` (default), the format is deduced from the filename extension, or from `ns.config['SAVE_FORMAT']` if there is none. As of now, *Novasoft* only supports the ASCII data format, which may be further modified by changing `ns.config['ASCII_FMT']`. As a special case, this module also contains functions to both save and load operation points files, see Section 2.3.3.
- **functions.py** defines commonly used higher-level operations for measurement scripts. Some examples include sampling an instrument and locking the local oscillator (LO) to some frequency. Helper functions take care of early error detection (*e.g.*, checking if a file is open for writing and if all values are in range) and define a common header format

	<b>Improving Band 9 Sensitivity by Advanced Tuning Algorithms — Final Study Report</b>	DocID: FEND-40.02.09.00-1944-C Version: C Date: 2020-01-07 Status: Released Page: 14 of 44
-----------------------------------------------------------------------------------	----------------------------------------------------------------------------------------------------	--------------------------------------------------------------------------------------------------------

for data files (see Section 2.3.2), among other things. Set `ns.config['PRINT_DATA']` to `True` to display data as it is measured. This is by far the largest module. Call `help` without an argument to print a list of available functions. Call `help(func)` to display that function's signature and docstring.

Each means of communication is represented by a separate module, which also serves as an example of how an instrument class could be implemented. Their docstrings refer to helpful resources. Users that want to use different types should implement their own instrument class, *i.e.*, one that inherits from `InstrumentBase`. Note that an instrument type object represents a single input (`readwrite='READ'`) or output (`readwrite='WRITE'`) channel. To read from and write to the same instrument, simply create two instrument type objects with the same address. The same goes for querying different properties from the same instrument.

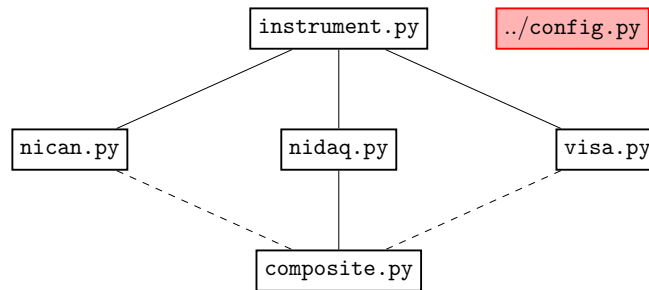


Figure 7: Structure of the `instruments` subpackage

The modules in the `instruments` subpackage:

- **`instrument.py`** provides common functionality for all instrument types. It implements a partially abstract base class `InstrumentBase`, which all instrument classes should inherit from. It also defines `InstrumentError`. When uncaught, such exceptions are automatically logged. Instrument objects have `val` (most recent value to be read or set) and `data` (list of all values since the last call to `instr.start`) attributes. Each child class can define `_connect`, `_start`, `_read`, `_write`, `_stop`, `_disconnect` and `_devices` methods. At the bare minimum, they should implement either reading or writing. The user should provide a name and a `readwrite` argument. Optional keywords arguments include `min_val`, `val` (initial value), `max_val`, `unit`, `average`, `step`, and `delay`. Every instrument object is then added to a dictionary, which is exposed to the user as `ns.instr.dict`.
- **`nican.py`** is the NI-CAN interface module, controlling the CAN-bus interface. It implements a class `NicanType`. Apart from the standard arguments, these devices should also specify a channel (e.g. `'CAN0'` or `'CAN1'`), a base address if it's the first CAN device on that channel, and a relative address. Furthermore, `unit` is required because it determines the number of bytes of data. Contrary to the case of *Rodrigo*, communication is automatically started once either `read` or `write` is called. All open CAN buses are automatically closed at interpreter termination time. To close a particular CAN port at an earlier point in time (e.g., to access it from a different program), one may use the static method `NicanType.shutdown(channel)`.
- **`nidaq.py`** is the NI-DAQmx interface module, controlling the analog/digital interfaces in the host computer. It implements a class `NidaqType`. Apart from the standard arguments, these devices should also specify an I/O type (`'ANALOG'` or `'DIGITAL'`) and a channel (e.g. `'Dev1/port10/line2'`). For brevity and familiarity with *Rodrigo*, two “aliases” `DacType` (analog I/O) and `LineType` (digital I/O) are defined. Meaning that

	<b>Improving Band 9 Sensitivity by Advanced Tuning Algorithms — Final Study Report</b>	DocID: FEND-40.02.09.00-1944-C Version: C Date: 2020-01-07 Status: Released Page: 15 of 44
-----------------------------------------------------------------------------------	----------------------------------------------------------------------------------------------------	--------------------------------------------------------------------------------------------------------

instead of writing `NidaqType(io_type='DIGITAL', ...)`, one can simply write `LineType(...)`. The same holds for analog I/O and `DacType`.

- **visa.py** is the VISA interface module, handling data communication over, *e.g.*, serial or GPIB interfaces. It implements a class `VisaType`. Apart from the standard arguments, these devices require a resource name (e.g. `'GPIB0::29::INSTR'`) and a command string (e.g. `'Pow %.3f dBm'`). As in the example, the latter should contain a replacement field if `readwrite` is set to `'WRITE'`. To facilitate the sending of other commands, *e.g.*, for configuring the instrument, `VisaType` also defines a `send(*commands)` function. If instead `readwrite` is set to `'READ'`, `data_type` should be set to either `'ASCII'` or `'BINARY'`. There are many other options described in the software documentation.
- **composite.py** defines more complex instrument types. For example, our measurement setup contains an optical chopper controlled through three NI-DAQmx lines, one to rotate the chopper wheel and two to determine its orientation. At this point in time, each composite instrument type (`ChopperType`, `MotorType`, `PaType`, `YigType`) is composed of a number of NI-DAQmx lines. This module also defines `DummyType`, which may be used for testing purposes.

## 2.3 Usage (as compared to *Rodrigo*)

Since the *Rodrigo* software has been around for a considerable amount of time, there is now a substantial collection of scripts, instrument configurations, data files, operation points files, and other related files (such as MATLAB scripts for inspecting scan data) involved. To preserve the value of these as much as possible, a balance had to be found between improving the software on one hand, and ensuring some level of compatibility and familiarity on the other. The remainder of this section illustrates the results of this effort.

### 2.3.1 Measurement scripts

The largest difference between *Rodrigo* and *Novasoft* is the fact that measurement scripts are no longer interpreted by custom lexer and parser code. Instead, measurement scripts are now fully-fledged Python scripts, which means that they can harness the full power of this high-level general-purpose programming language. As these scripts are executed directly, we must now add a few lines of code for importing the *Novasoft* libraries and for initializing the setup. Alternatively, one could start an interactive Python session (either from a command prompt or through an IDE like Spyder), enter the import/init statements once, and then control the setup either line by line or by using, *e.g.*, the built-in `execfile` function to run one or more measurement scripts. This has the added benefit of remembering the state of the setup: if script 1 sets an instrument to some value, script 2 will also know about it. (Note that in *Rodrigo*, the very same function was fulfilled by the GUI.)

Resemblance to the old syntax was maintained as closely as possible, but without sacrificing quality and ease of use. Some differences stand out immediately. For example, all functions now adhere to the Python syntax for functions calls, namely function name + open parenthesis + comma-delimited (keyword) arguments + close parenthesis. Other changes, such as the removal of semicolons and the addition of quotation marks around strings, are more subtle. This report does not contain a full list of changes. For details, please refer to *Novasoft*'s documentation.

	<b>Improving Band 9 Sensitivity by Advanced Tuning Algorithms — Final Study Report</b>	DocID: FEND-40.02.09.00-1944-C Version: C Date: 2020-01-07 Status: Released Page: 16 of 44
-----------------------------------------------------------------------------------	----------------------------------------------------------------------------------------------------	--------------------------------------------------------------------------------------------------------

Here follow some code snippets as examples:

*Rodrigo* (using an instrument configuration file that has been loaded by the GUI):

```

1 # Take measurements
2 read Tcr4K;
3 set CHOPPER 1;
4 send HPMETER_POL0 {OUTPUT:REC1:STAT OFF};
5 sample(filename.dat, 300, 0.1, GET_POLO_MIXER_TEMP, GET_POL1_MIXER_TEMP,
6     GET_4K_STAGE_TEMP, GET_20K_STAGE_TEMP, GET_90K_STAGE_TEMP);
7 1Dscan(filename.dat, SET_POLO_SIS1_JUNCT_V, -8, 0.01, 8, 0.01,
8     GET_POLO_SIS1_V, GET_POLO_SIS1_C);

```

*Novasoft* (using an instrument configuration file):

```

1 import numpy as np
2
3 import novasoft as ns
4 from novasoft.functions import * # read, set, send, sample, scan1D, ...
5
6 # Initialize
7 instr_dict = ns.load_cfg('Cartridge_Config.cfg') # Tcr4K, CHOPPER, HPMETER_POL0, ...
8 globals().update(instr_dict)
9
10 # Take measurements
11 read(Tcr4K)
12 set(CHOPPER, 1)
13 send(HPMETER_POL0, "OUTPUT:REC1:STAT OFF")
14 sample('filename.dat', 300, 0.1, GET_POLO_MIXER_TEMP, GET_POL1_MIXER_TEMP,
15     GET_4K_STAGE_TEMP, GET_20K_STAGE_TEMP, GET_90K_STAGE_TEMP)
16 scan1D('filename.dat', SET_POLO_SIS1_JUNCT_V, np.linspace(-8, 8, 1601), 0.01,
17     GET_POLO_SIS1_V, GET_POLO_SIS1_C)

```

*Novasoft* (without using an instrument configuration file):

```

1 from novasoft.functions import *
2 from novasoft.instruments import NicanType, ChopperType, VisaType
3
4 # NI-CAN (note: base_addr is only specified once per channel)
5 GET_SETUP_INFO = NicanType(name='GET_SETUP_INFO', readwrite='READ', unit='u',
6     channel='CAN0', base_addr=0x13, rel_addr=0x20001)
7 GET_POL1_MIXER_TEMP = NicanType(name='GET_POL1_MIXER_TEMP', readwrite='READ',
8     unit='K', channel='CAN0', rel_addr=0x48d0)
9
10 # NI-DAQmx (composite instrument type containing three NI-DAQmx lines)
11 CHOPPER = ChopperType(name='CHOPPER', readwrite='WRITE', min_val=0, max_val=1,
12     chop_line='Dev1/port10/line1',
13     sensor1='Dev1/port6/line7', sensor2='Dev1/port6/line6')
14
15 # VISA
16 temp_sett = {'readwrite': 'READ', 'unit': 'K', 'rsrc_name': 'GPIB0::12::INSTR',
17     'data_type': 'ASCII', 'timeout': 3}
18 Tcr4K = VisaType(name='Tcr4K', command_str="KRDG? 5", **temp_sett)
19 Tcr12K = VisaType(name='Tcr12K', command_str="KRDG? 6", **temp_sett)
20 Tcr90K = VisaType(name='Tcr90K', command_str="KRDG? 7", **temp_sett)
21 Troom = VisaType(name='Troom', command_str="KRDG? 8", **temp_sett)
22
23 # Take measurements
24 ...

```

 <p>NOVA Sub-mm Instrumentation Group</p>	<p><b>Improving Band 9 Sensitivity by Advanced Tuning Algorithms — Final Study Report</b></p>	<p>DocID: FEND-40.02.09.00-1944-C Version: C Date: 2020-01-07 Status: Released Page: 17 of 44</p>
------------------------------------------------------------------------------------------------------------------------------------	-----------------------------------------------------------------------------------------------------------	-------------------------------------------------------------------------------------------------------------------

### 2.3.2 Data files

In Section 2.2, it was explained that the new infrastructure allows measurement data to be saved in one of several formats. One problem with *Rodrigo*'s ASCII files is their unnecessarily complex structure. They were designed with humans in mind rather than computer programs. Another problem is the inconsistency between data files originating from different scan functions. For example, files from a two-dimensional scan look completely different than those coming from an optimization routine. In *Novasoft*, all headers consist of a number of `key:value` pairs preceded by a comment sign. The header is followed by an uninterrupted stream of data points. This means that they can be loaded using `numpy.loadtxt`. Note that a new format specifier can be set by modifying `ns.config['ASCII_FMT']`.

### 2.3.3 Operation points files

The `ns.optimize` function finds optimum bias voltage and LO power settings for different LO frequencies (described in section 3.2). Several other functions require these operation points to achieve relevant results. Therefore, the result of `optimize` can be saved to a file. In *Rodrigo*'s case, a MATLAB script turns the raw data into an operation points file. In *Novasoft*'s case, `optimize` saves the raw data but returns the optimum settings, which can be passed to `ns.save_operation_points`. The format of these files has also changed. They now look similar to data files, although they have some additional restrictions. The first column must contain LO frequencies. The remaining columns contain the corresponding optimum settings (albeit not necessarily bias voltages and LO powers). Optionally, the user can pass a `s2g_dict` argument to `save_operation_points`. If done so, the last two columns will later be passed to `ns.set_to_get` as initial guesses and goal values, respectively. This was implemented because what we actually want to set is some bias current, but this can only be achieved by tuning the drain voltage of the LO's power amplifier.

	<b>Improving Band 9 Sensitivity by Advanced Tuning Algorithms — Final Study Report</b>	DocID: FEND-40.02.09.00-1944-C Version: C Date: 2020-01-07 Status: Released Page: 18 of 44
-----------------------------------------------------------------------------------	----------------------------------------------------------------------------------------------------	--------------------------------------------------------------------------------------------------------

### 3 The old algorithms

The Band 9 receivers that have been installed in ALMA were tuned with the help of two algorithms. One to tune the magnet current and one to find optimal SIS bias voltages and currents (controlled by LO power) for each LO frequency. The latter was implemented in the old *Rodrigo* measurement software [8], while the former was performed mostly by hand. They serve as a benchmark for the advanced tuning project.

#### 3.1 Magnet current

The basic algorithm for the magnet tuning, which was up to now largely performed by hand and eye, is as follows:

- Measure a Josephson current “suppression curve” as theoretically shown in Figure 1;
- Locate the minima;
- Pick the magnet current corresponding to a low, stable (wide, smooth) minimum, which usually turns out to be the second;
- Check the actual suppression level in an IF power vs. SIS bias voltage plot. If this looks okay, we are done and ready to move on to the next tuning step.

The *actual* magnet tuning algorithm is more complicated than that, for two reasons.

In the first place, in order to measure a representative IF power versus bias voltage curve, the local oscillator must be turned on. Otherwise, there will be no IF power to measure, nor will any Shapiro steps appear. This means that some LO power must be applied, leading to a certain bias current in the I–V curve of the mixer. The frequency of this LO signal is rather arbitrary, and we use 690 GHz in practice. After that, defining a suitable bias current only makes sense at a specific bias voltage. Therefore, we must first set  $V_{bias}$  and  $I_{bias}$  before we can tune  $I_{mag}$ . Their initial values are based on earlier tunings of other mixers. It was found that  $I_{bias} = I_{gap}/5$  at  $V_{bias} = 2$  mV tends to be a good guess for Band 9 DSB receivers.

The second complication is that the Josephson suppression does not only depend on the magnetic flux generated by the superconducting coil, but also on any flux trapped in the SIS junction. Varying amounts of trapped flux make it impossible to use a simple look-up table for magnet operation, as clearly visible in Fig 8. To get the same suppression curve each time, one should first expel the trapped flux, which is done by a combined degaussing-defluxing procedure. As mentioned before in the introduction, however, this procedure is not successful every time. Therefore, during qualification, we must repeat this procedure several times and pick the “most common” result. If different curves keep turning up, the mixer is rejected for production. Since only a limited number of tries can be executed during commissioning, there is no hard guarantee however that once deployed the mixer will never end up in an abnormal suppression regime.

To illustrate, a typical mixer tuning cycle looks as follows:

We start by determining the gap current  $I_{gap}$ . This is most easily achieved with the LO off. We measure its I-V characteristic from 0 to 8 mV and determine the gap current afterwards by a Matlab script (Fig. 9).

The next step is to measure the Josephson suppression curve. For that, we have to expel trapped flux from the junction, the so-called demag-deflux cycle mentioned before. This process

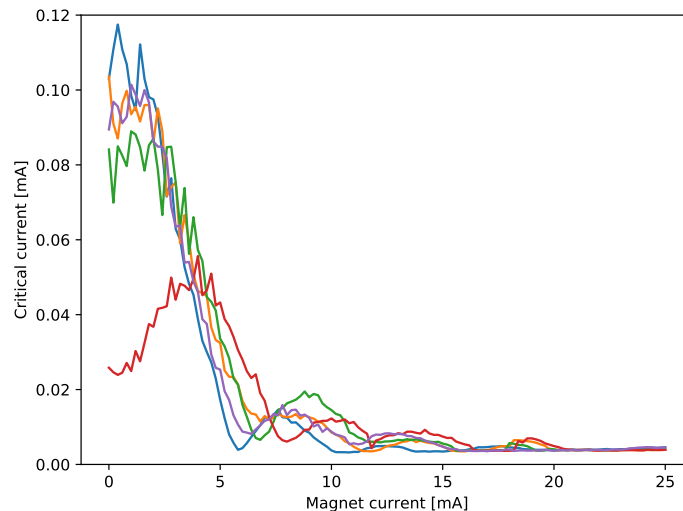


Figure 8: Critical Josephson current versus magnet current after trapping different amounts of magnetic flux. Without applying a degaussing procedure, the curves do not overlap.

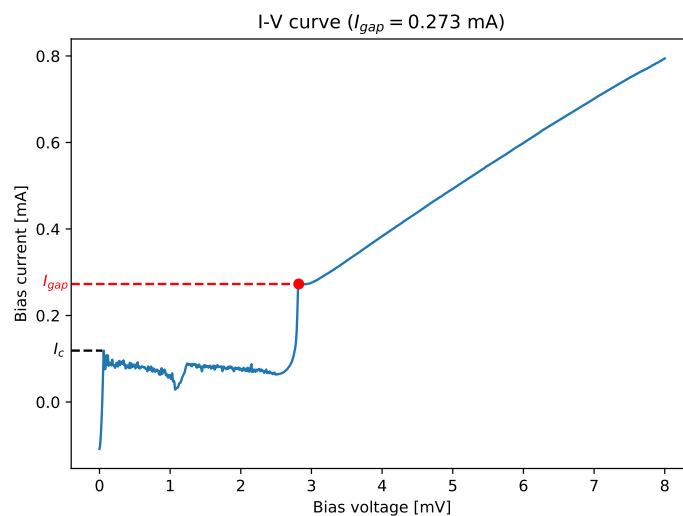


Figure 9: Identifying the gap current, used to determine a suitable pump current.

consists of two steps. First, we demagnetize (degauss) the core of the magnet by applying a slowly alternating current of decreasing amplitude. This randomizes the orientation of its magnetic domains, resulting in a net near-zero field. Secondly, we give a heater pulse to temporarily lift the mixer temperature above the critical temperature. Because of the Meissner effect, cooling the superconducting films through  $T_c$  at zero field should expel most of the flux. Then, the magnet current is slowly increased from 0 to 25 mA, in small increments (in this case 0.2 mA steps, in later implementations we used 0.1 mA). At each magnet current, a small I–V curve around zero bias is recorded, and half the current step at around zero bias is taken as the critical current (Fig 10).

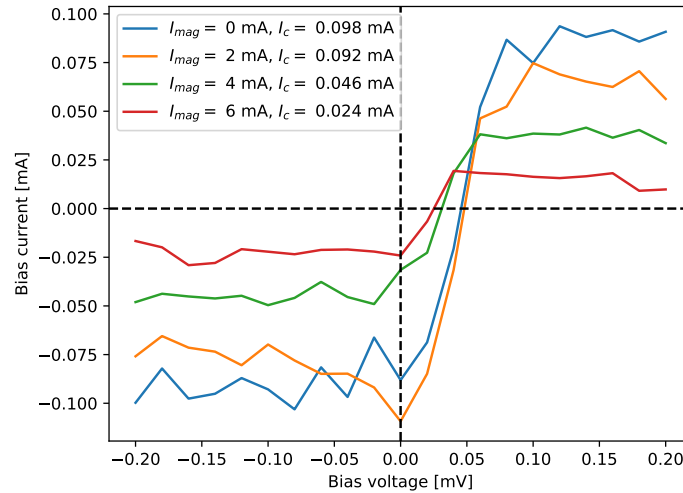


Figure 10: Determining  $I_c = (I_{max} - I_{min})/2$  at several magnet currents by small bias voltage sweeps around zero. The offsets on both bias voltage and current are artefacts of the read-out electronics and are compensated by the software.

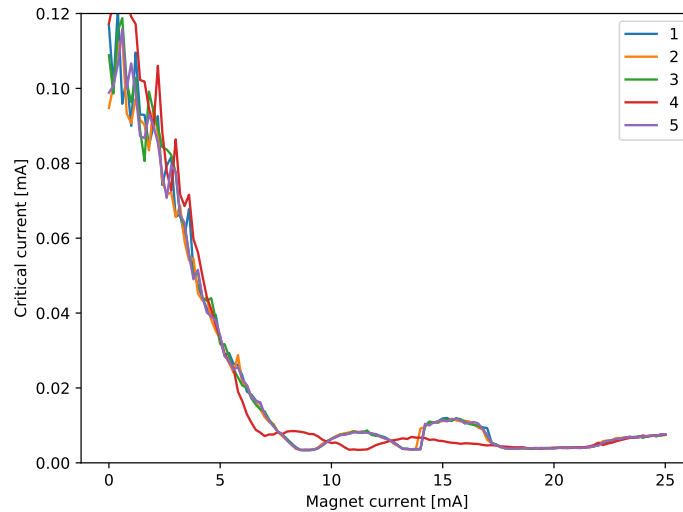


Figure 11: Five consecutive sweeps of critical Josephson current versus magnet current, each taken after a fresh degaussing/defluxing cycle.

Because the demagnetization and defluxing procedure does not always succeed at eliminating trapped flux, we repeat this process five times and thus obtain five  $I_c$  versus  $I_{mag}$  curves (Fig. 11).

Clearly, the fourth time the junction ended up in a different state. During production, that was reason enough to reject a mixer. For now, we ignore that curve and determine the minima of the remaining curves. In this case, the first minimum is lower and broader than the second one, which is rare for Band 9 mixers. It occurs at  $I_{mag} = 8.8$  mA.

Once this is determined, we demagnetize/deflux once more because the high magnet currents occurring as part of the sweep are likely to introduce fresh trapped flux, leading to an invalid

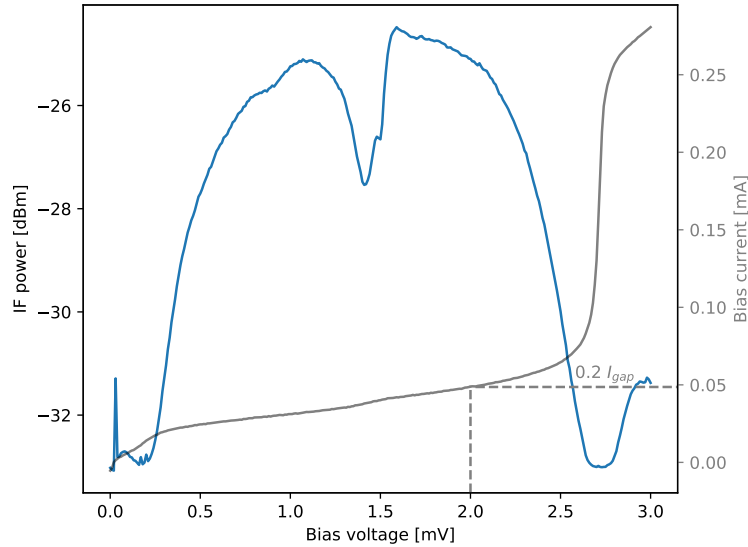


Figure 12: IF power versus bias voltage after applying the optimum magnet current and a certain LO power. Also shown is the final I–V curve. The LO power is such that  $I_{pump} = I_{gap}/5$  at  $V_{bias} = 2$  mV.

suppression regime. After this, we set the chosen magnet current, making sure never to exceed this value by a substantial amount, for the same reason. Lastly, we apply some LO power and check the actual suppression level. This is done by way of an IF power vs. SIS bias voltage scan, as shown in Fig. 12.

In this case, we achieved a good result, and the resulting  $I_{pump}$  and  $I_{mag}$  can be saved for later use. In cases where the IF power vs. bias voltage curve does not look clean, we can try a different (higher order) minimum.

In the final acceptance of a magnet tuning, especially the width of the Josephson region is important. The region must be narrow enough to leave sufficient room for finding a stable bias voltage without compromising the IF power and hence noise temperature too much. Since this is difficult to quantize, during Band 9 production a simpler criterion was used, namely that the total amplitude of the Josephson feature must be below a certain value (6 dB in practice) and its width smaller than 0.4 mV. The downside of this fast check is that probably a fair number of excellent mixers were rejected undeservedly. At the time, pressure on the delivery schedule drove the acceptance of this simplified procedure.

### 3.2 Bias voltage and LO power (operation points)

Determining the Josephson suppression field is the most critical part of the tuning procedure. Compared to that, finding optimal bias voltages and LO powers is relatively straightforward. We sequentially set the LO frequency to a series of values (typically 614 . . . 710 GHz in 8 GHz increments). At each frequency, we scan the bias voltage and the drain voltage of the LO's power amplifier (which controls its output power) over some reasonable range and determine the resulting noise temperature by a hot-cold measurement. We pick the values that correspond to the lowest noise temperature (or in practice, in the case of  $V_{bias}$ , the highest IF power, which

	<b>Improving Band 9 Sensitivity by Advanced Tuning Algorithms — Final Study Report</b>	DocID: FEND-40.02.09.00-1944-C Version: C Date: 2020-01-07 Status: Released Page: 22 of 44
-----------------------------------------------------------------------------------	----------------------------------------------------------------------------------------------------	--------------------------------------------------------------------------------------------------------

is strongly correlated to the noise temperature and also a better predictor for the stability).

The Josephson region itself must explicitly be excluded from the possible range of bias voltages. Other unsuitable regions (close to the left end of the first photon step ( $\approx 0.14$  mV) or to the gap voltage ( $\approx 2.8$  mV) are automatically excluded as there is little IF power available there. The width of a Josephson region depends on  $V_{AC}$ , the induced voltage swing over the junction, and thus on the temperature of the black body radiators used for the hot/cold measurements. This means that for some bias voltages,  $V_{bias, hot}$  may lie inside the Josephson region (leading to much higher values) while  $V_{bias, cold}$  does not. In these cases, extremely low and even negative noise temperatures may be observed, but these should obviously be considered to be artefacts. To be on the safe side, we filter out bias voltages with Y-values smaller than 1.05 ( $T_{noise} = 4383$  K) and within 0.4 mV of any Shapiro step situated at  $V_{DC} = n \frac{h\nu}{2e}$ , with  $\nu$  the LO frequency.

The following series shows how a typical tuning sequence looks in practice (repeated for the chosen set of LO frequencies):

- A demag-deflux cycle is performed and the magnet set to the chosen suppression current;
- The bias voltage is set to a fixed value of 2 mV;
  - The LO power  $P_{LO}$  is swept (by way of its drain voltage), both looking at a hot and a cold load, and the LO power of minimum noise temperature determined from the resulting Y-factor (Fig. 13);
  - At this LO power setting, the SIS bias voltage  $V_{bias}$  is swept, and the point of highest IF power determined, excluding the regions around the first and second Shapiro steps (Fig. 14). For comparison, the corresponding noise temperatures are shown in Fig. 15;
  - The bias voltage is set to the found optimum;
- The last three are repeated once more to converge to an optimal  $(V_{bias}, P_{LO})$  pair;

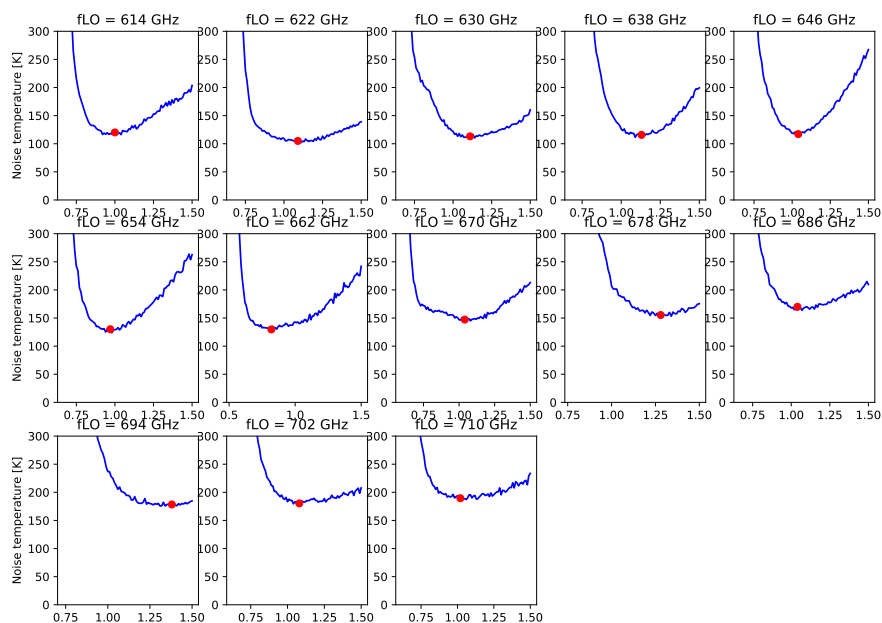


Figure 13: Noise temperature versus drain voltage of the LO’s power amplifier. The red circles denote the optimum LO powers, corresponding to the lowest noise temperature. The resulting bias current (not shown) is stored rather than the drain voltage itself.

- Finally, after tuning the mixer this way for each LO frequency, it is again defluxed and the optimum settings applied. Then the noise temperature as a function of LO frequency is measured (Fig. 16), followed by other performance verifications (stability, compression, cross-talk, etc.).

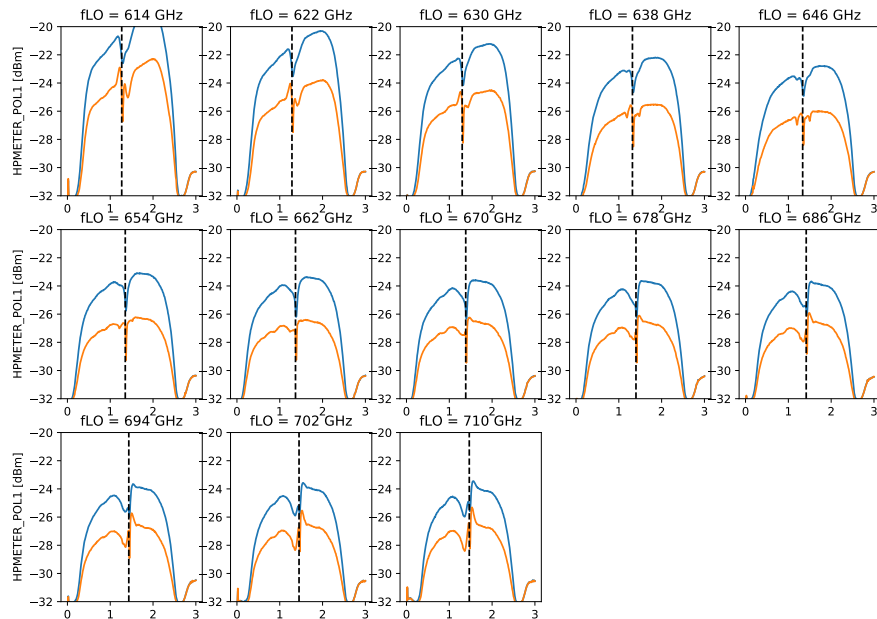


Figure 14: IF power versus bias voltage for a hot (295 K, blue) and a cold (77 K, orange) load. From these curves,  $T_{noise}$  values can be computed. Dashed line: first Shapiro step.

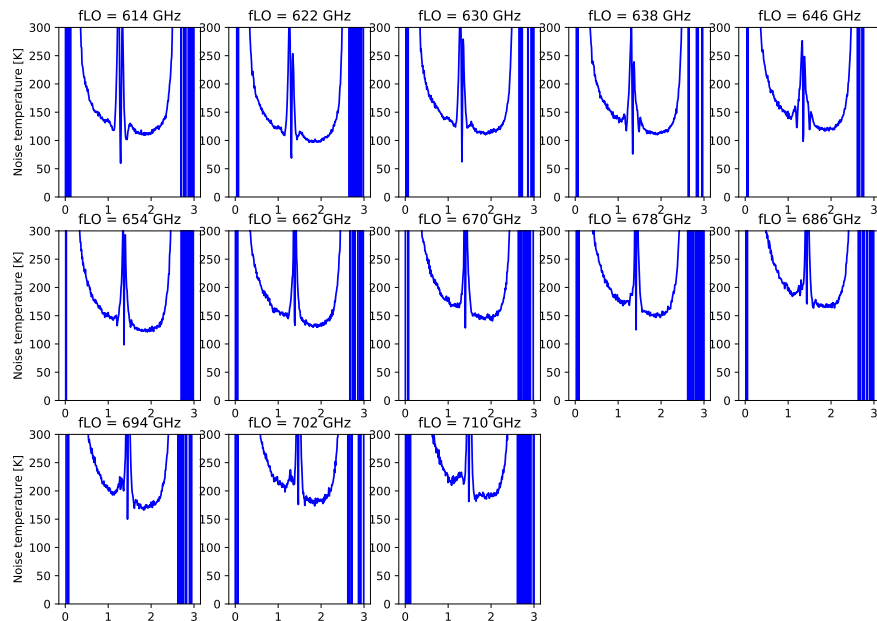


Figure 15: Noise temperature versus bias voltage, determined by Y-factor formula from the data in Fig. 14

As can be seen in Fig. 16, we have obtained good results for polarization 0, while polarization 1 is just barely within spec. The main goal of the current study is to improve this sensitivity.

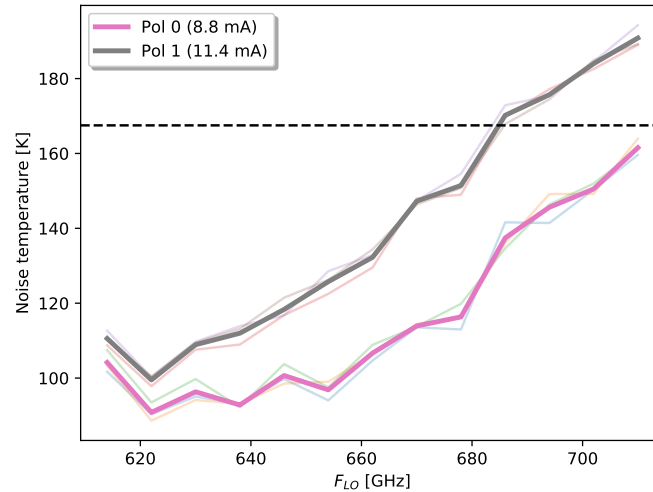


Figure 16: The final noise temperatures achieved with the two mixers in one cartridge. The thick lines mark the average of three consecutive measurements. The consistent results already give an indication of stability and repeatability. The ALMA specifications state that 80% of the curve should be below the dashed line at 168 K (and 100% below 250 K).

Note that to fully characterize a tuning, one must also measure the resulting power stability and gain compression.

### 3.3 Mixer qualification

During qualification of the Band 9 mixers for delivery, the procedure described in the previous section was generally followed. On the way, there were several decision points where a mixer could be rejected. The decision sequence is briefly summarized here:

- Repeat the following steps five times:
  - Demagnetize and deflux the mixer;
  - While sweeping the magnet current from 0 to 25 mA, record the critical current by taking small bias scans around 0 mV;
- If the five resulting curves are not identical, reject the mixer. Small deviations are sometimes allowed if they don't interfere with the minima.
- Select the desired minimum (typically the second one);
- Repeat the following steps three times:
  - Set bias voltage and LO power to zero;
  - Demag and deflux;
  - Set the magnet to the current for the selected minimum;
  - Bias the mixer at a fixed voltage (typically 2 mV) and apply LO power (at 690 GHz) to bring the pumping current up to 20% of the gap current;
  - Measure the IF power as function of SIS bias voltage. If the Josephson feature is larger than 6 dB peak-peak or wider than 0.4 mV, reject the mixer.
- If the preceding three cycles do not yield the same results, reject the mixer.
- Test the mixer against all performance specifications (noise temperature, gain stability, gain compression, etc.). Reject the mixer if one of the specifications is not met (or can not be waived after discussion with the client).

 <p>NOVA Sub-mm Instrumentation Group</p>	<p><b>Improving Band 9 Sensitivity by Advanced Tuning Algorithms — Final Study Report</b></p>	<p>DocID: FEND-40.02.09.00-1944-C Version: C Date: 2020-01-07 Status: Released Page: 25 of 44</p>
------------------------------------------------------------------------------------------------------------------------------------	-----------------------------------------------------------------------------------------------------------	-------------------------------------------------------------------------------------------------------------------

## 4 Automating the tuning algorithm

Now that the traditional tuning procedure, based on human decisions, has been outlined, the question is how to automate this process fully, and potentially improve it. The primary goal is to apply it at the front end, to optimize the performance in a much more refined way than can be obtained with the traditional table-driven method. Very likely, an additional benefit is the reduction of operator's time both in daily operations as well as in establishing new reference values (*e.g.*, when conditions change due to aging front-end coolers). In the following sections, we describe the steps we have taken to arrive at a fully automated determination of the magnet current.

In essence, the tuning algorithm is still largely following the time-proven algorithm described in section 3. However, the main suppression sequence now consists of two subparts: an initial determination of the magnet current based on the critical current in the mixer, and a refinement and verification based on the Josephson feature in the IF power vs. bias voltage curve.

Before the suppression current can be determined, a demagnetization-defluxing cycle has to be performed and the gap current to be determined in order to set a reasonable initial pumping level.

### 4.1 Demag-deflux cycle

In order to minimize the time needed for the optimizing routine, one algorithmic aspect to investigate was the influence of the demag-deflux parameters (especially the timing) on the suppression, as we found that this may not be negligible. For this, the demag-deflux sequence was tried for different values for the maximum magnet current, current step and dwell time, and heater pulse length.

It turned out for the demagnetization procedure, a pattern of alternating positive, zero, negative and again zero currents with decreasing magnitude in each cycle gave the most repeatable results. The magnitude of the current should decrease from 50 mA with 1 mA steps per cycle, each with a dwell time of 0.1 s. We do not have a ready explanation for these particular values, but it is likely that the remanent magnetic field of the core and the self inductance of the coil play a major role.

The length of the deflux heater pulse was fixed at 0.5 s, which is amply sufficient to get the junction out of superconductivity. We found that when the heater pulse is reduced too far below this value, the heater might not work at all, probably because of software delays in the M&C unit and R-C times in the electronics; half a second was chosen as a safe value. All in all, the demag-deflux cycle takes about 30 seconds.

### 4.2 Determining the gap current

The gap current (*i.e.*, the junction current when biased just above the gap voltage) is needed in an early stage of the algorithm to set a reasonable LO pumping level for the Josephson suppression procedure. Later, after good suppression is obtained, the final pumping level is determined in the conventional way by optimizing the noise temperature.

A robust method to determine the gap voltage and current was developed during the years of

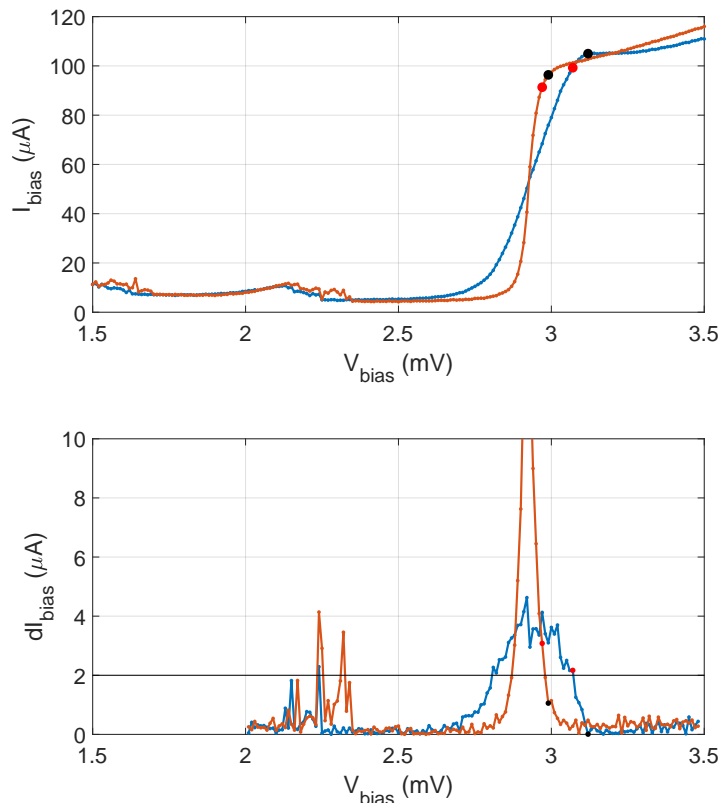


Figure 17: I-V curves of two typical mixers, one with a clear series resistance (top panel) and their numerical derivatives (bottom panel). The derivatives are used to find the gap voltage (close to the top of the gap) and corresponding current. The red and black dots represent the initial and final approximations, as described in the text.

working with the ALMA receivers. Even when there is a normal resistance in the mixer it is still possible to find reliable values this way.

The method is demonstrated in Fig. 17 for two different mixers, one having a considerable series resistance. An unpumped I-V curve is recorded at 0 mA magnet current (upper panel), and the absolute differences in current between successive points are determined (lower panel). The last point with a current difference above a threshold of  $2 \mu\text{A}$  is determined (red dots in the graph), after which the next minimum in current difference is taken as the gap voltage (black dots). Finally, the gap current is derived from this voltage using the original I-V curve, shown in the upper graph as black dots again. As can be seen in the graph, this simple algorithm has a tendency to “catch” on noise excursions, but it is accurate enough for the purpose of finding a pumping level suitable for determining the parameters of the Josephson feature. For other purposes where more accuracy is needed, some filtering could be applied beforehand.

### 4.3 Determining the critical current

The traditional procedure to determine the critical current as described in section 3.1 was simplified. Instead of taking a small I-V curve around zero bias for each magnet current, and

	<b>Improving Band 9 Sensitivity by Advanced Tuning Algorithms — Final Study Report</b>	DocID: FEND-40.02.09.00-1944-C Version: C Date: 2020-01-07 Status: Released Page: 27 of 44
-----------------------------------------------------------------------------------	----------------------------------------------------------------------------------------------------	--------------------------------------------------------------------------------------------------------

finding the extrema in it, we now simply take the difference between two points measured just below and above the zero-crossing (typically  $\pm 0.2$  mV), respectively. Although the result is more noisy than the original method (especially at very low magnet currents), it is much faster and still yields stable enough results around the suppression minima to determine the latter accurately.

#### 4.4 Obtaining the initial suppression point

The first attempt at determining the suppression points, based on a numerical differentiation of the entire suppression curve, is described in the Midterm Review Report[5] section 3.3.2. We abandoned this approach for several reasons, mainly the time it takes and the probability of introducing new flux in the mixer or remanent field in the core by going to high magnet currents.

Instead, we now simply start at a low magnet current (typically 0 mA, but this could be higher if a specific minimum is sought after) and increase the current in small steps until a minimum is passed (filtered for noise). At this moment we stop, and the current value with the smallest critical current value is taken as initial point for the refinement.

#### 4.5 Refining the suppression

After the first minimum of the critical current is found, the suppression is refined by minimizing the weight of the Josephson feature in the IF power vs. SIS bias characteristic of the mixer, as function of magnet current, while applying mixer bias voltage and LO power at a fixed frequency.

The weight of the Josephson feature is determined by integrating the IF power over a small range ( $V_J + 0.05$  mV to  $V_J + 0.15$  mV, in steps of 0.01 mV), as show by the black section in the curves of figure 18. The center of the Josephson feature,  $V_J$ , follows from the LO frequency ( $V_J = F_{LO}/484$ ). These integrations are done while the magnet current is changed in small steps from the initial value found in the previous section, in both negative and positive directions. The magnet current in this range with the smalled Josephson power is taken as the candidate for the refined value, which now has to be tested for usefulness.

Note added following up on concerns raised at the review, and after some experimentation: in order to prevent a strong negative central part of the Josephson feature to reduce the integral substantially, and thereby increasing the probability of flagging a minimum with a small likelihood to be qualified, we suggest to move the integration interval slightly upwards (say,  $V_J + 0.1$  mV to  $V_J + 0.2$  mV).

#### 4.6 Verifying the suppression

The usability of the candidate suppression point is tested by requiring the *width* of the Josephson feature to be below a certain value. Thus turns out to be a robust criterion, more so than the *height* of the feature that was used during Band 9 mixer qualification. Up to now, this method worked well for 11 tested mixers (two of which had an aluminum oxide barrier, the rest aluminum nitride).

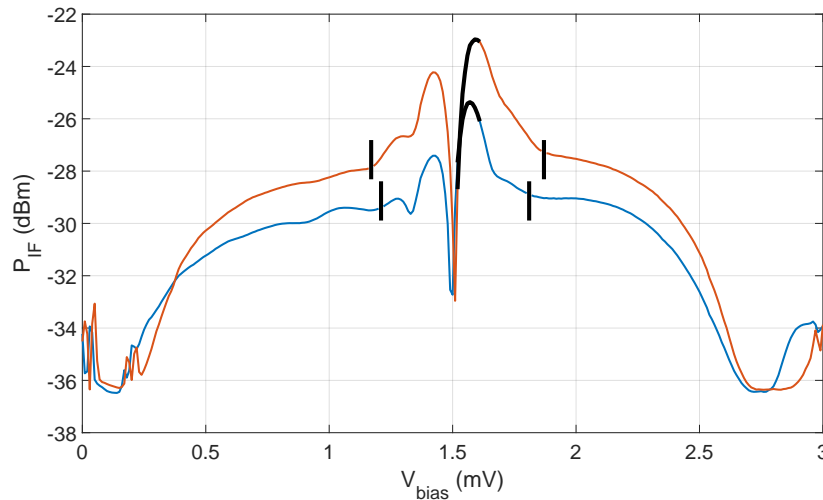


Figure 18: The IF power as function of mixer bias voltage for two different mixers. The Josephson feature consists of the central dip with adjacent peaks. The integration interval used to determine the size (weight) of the Josephson feature is indicated in black. The little vertical bars left and right of the Josephson feature denote the limits of the latter found by the refinement part of the tuning algorithm.

The width is determined by numerically differencing the power while moving the bias voltage both up and down from the nominal Josephson voltage, as follows: starting from  $V_J$ , we first increase the voltage with steps of 0.01 mV until the difference with the previous power reading is below 0.05 dB for 10 consecutive points. This we consider the upper extent of the Josephson peak; the lower extent is determined in the same way by decreasing the voltage. Finally, we define the width of the Josephson feature as the difference between the upper and lower extents.

If this peak width is now smaller than a certain value, we consider the suppression to pass the test. For the value of the upper limit, we have chosen 0.8 mV because this gives reliable results while still leaving sufficient space to bias the mixer outside the Josephson peak.

If the first minimum doesn't yield a peak width below the specified threshold, the magnet current will be increased until the next minimum is found, past the first encountered maximum of course. Note that the search for the next minima is purely based on the Josephson IF power, not on the critical current. This will be repeated until the peak width is below the given threshold, or the magnet current reaches a pre-set limit (we chose 25 mA), at which it must be concluded that the mixer cannot be tuned this way. None of the eleven tested mixers failed in this respect, as each yielded a qualified minimum.

## 4.7 The final tuning algorithm

Putting all the parts discussed above together, we arrive at the following algorithm for Josephson suppression.

1. Set the bias voltage and magnet current of the mixer to be defluxed to zero. Turn the LO power OFF.
2. Apply a demagnetization sequence to the magnet. This consists of a consecutive series of

	<b>Improving Band 9 Sensitivity by Advanced Tuning Algorithms — Final Study Report</b>	DocID: FEND-40.02.09.00-1944-C Version: C Date: 2020-01-07 Status: Released Page: 29 of 44
-----------------------------------------------------------------------------------	----------------------------------------------------------------------------------------------------	--------------------------------------------------------------------------------------------------------

current settings to the magnet, starting at a high positive value, and oscillating between positive and negative values, while reducing their magnitude to zero. The recommended sequence is (with 0.1 s. dwell times at each current level): +50 mA, 0, -50 mA, 0, +49 mA, 0, -49 mA, 0, +48 mA, 0, -48 mA, 0, ..., +1 mA, 0, -1 mA, 0 mA.

3. Apply a deflux pulse to the mixer heater: 24 V (fixed-voltage) for 0.5 s. And wait for the mixer to cool down to 10% above its original temperature.
4. Minimize the critical current by increasing the magnet current with steps of  $dI_{step} = 0.1$  mA:
  - a. Increase the magnet current with  $dI_{step}$  starting from  $I_{initial}$ .
  - b. At each step measure the bias current at -0.2 and 0.2 mV bias voltage and determine the difference ( $I_{critical}$ ).
  - c. While  $I_{critical}$  is decreasing go to 4a.
  - d. If  $I_{critical}$  is minimum go to 5, else go to 4a.
5. Tune the magnet by minimizing power at Josephson peak:
  - a. Put the LO frequency at 710 GHz (no locking needed)
  - b. Put  $V_{bias}$  at 2.0 mV and increase the LO power until  $I_{bias}$  is 20% of the gap current.
  - c. Integrate the power over  $V_J + 0.05$  to  $V_J + 0.15$  with steps of 0.01 mV; this results in  $P_{integrate}$ .
  - d. Change the magnet current in both directions with  $dI_{step}$  until the minimum  $P_{integrate}$  is found. First in negative direction, then the positive direction.
  - e. If the peak width is below the threshold of 0.8 mV the tuning is done else go to 5f.
  - f. Increase the magnet current with  $dI_{step}$  until the maximum  $P_{integrate}$  is found. (Go over the maximum to get the next minimum)
  - g. Increase the magnet current with  $dI_{step}$  until the minimum  $P_{integrate}$  is found.
  - h. If the peak width is below the threshold of 0.8 mV the tuning is done else go back to 5f.

The minimum/maximum in the algorithm is found when it stays minimum/maximum for 5 following magnet steps. This is to filter out spikes and local minima/maxima.

## 4.8 Application of the algorithm

There are several ways the tuning algorithm could be applied in practice. One way is simply to run it every time the receiver is started up, trusting that the algorithm finds good operating points (or flag an error if it doesn't). Since each suppression attempt takes a certain amount of time, this could adversely influence the time needed to switch between bands. Another possibility is to prepare a database of initial settings for each mixer to speed up the search for the best minimum. In addition, a set of reference tunings could be stored for quick comparison, to ensure that each time the mixer is tuned it is in the *same* operating point rather than any "random" point that fulfills the requirements, which could be beneficial for reproducibility of calibrations, etc.

To test the merits of the approach sketched above, we performed repeatability test on a set of eleven mixers (two of which were of  $\text{AlO}_x$ -barrier type). Initially, the algorithm was run 20 times on each mixer, starting from  $I_{initial} = 0$  mA. From the resulting magnet currents the median was taken and this is considered the "optimum" magnet current  $I_{opt}$ . Figure 19 shows two examples: one mixer (right panels) arrived at the same suppression each time, while for the other (left panels) several solutions were found. Note that, apart from a possible extra requirement of reproducibility, all suppressions of the second mixer can be considered valid, as they all meet the Josephson-width criterion.

	<p><b>Improving Band 9 Sensitivity by Advanced Tuning Algorithms — Final Study Report</b></p>	<p>DocID: FEND-40.02.09.00-1944-C Version: C Date: 2020-01-07 Status: Released Page: 30 of 44</p>
-----------------------------------------------------------------------------------	-----------------------------------------------------------------------------------------------------------	-------------------------------------------------------------------------------------------------------------------

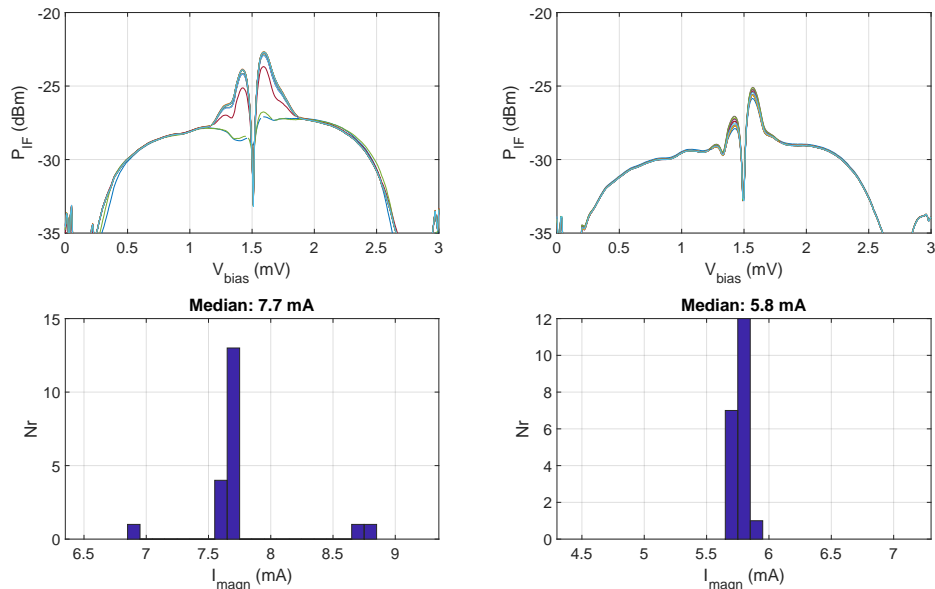


Figure 19: The tuning algorithm applied 20 times in a row to two different mixers: on top the resulting IF power vs. bias voltage curves, below a histogram of the found magnet currents. The left mixer arrives at three different solutions (all valid in principle), while the right consistently ends up in the same point.

After this, to simulate real operation, the tuning algorithm was applied five times for each mixer, starting 1 mA below this optimum magnet current:  $I_{initial} = I_{opt} - 1$  mA and stopping at  $I_{opt} + 1$  mA. A deviation of 0.2 mA from the original found optimum magnet current is allowed to qualify this as a repeatable tuning. For eight mixers out of these eleven it turns out that the optimum is reached at the first attempt each time. For three mixers, a few times, it took two or even three attempts to get to the predetermined magnet current.

For the operational Band 9 mixers in ALMA it is expected that almost all will tune within one attempt, because those mixers were already selected for repeatability using the traditional tuning methods. In this case, in the current form of the algorithm, the full tuning cycle takes about 50 seconds to complete, of which the demag-deflux cycle takes 30 seconds. Note that the full tuning is only needed when switching from “Off” to “Standby” mode, adding 20 seconds to the traditional procedure (assuming it is successful in the first attempt). As long as the cartridge is kept in “Standby” mode, it is unlikely that retuning is needed. Also note that, since the suppression currents are independent of the LO frequency (as will be demonstrated in section 5.5.3), re-running the tuning algorithm should not be necessary when changing the observation frequency within the band.

#### 4.9 Selecting an arbitrary minimum

If for some special reasons (increased compression level comes to mind) it is desired to select a higher minimum than the first qualifying one, two solutions are suggested.

For the purpose of simply ending up with a higher suppression current, a higher starting current for the initial minimum search (step 4 of the algorithm) can be chosen. The first qualifying minimum found is then guaranteed to be above this current.

 <p>NOVA Sub-mm Instrumentation Group</p>	<p><b>Improving Band 9 Sensitivity by Advanced Tuning Algorithms — Final Study Report</b></p>	<p>DocID: FEND-40.02.09.00-1944-C Version: C Date: 2020-01-07 Status: Released Page: 31 of 44</p>
------------------------------------------------------------------------------------------------------------------------------------	-----------------------------------------------------------------------------------------------------------	-------------------------------------------------------------------------------------------------------------------

Alternatively, if a minimum of or above a certain *order*, say  $N$ , is desired, step 5e of the algorithm could be modified to “artificially” fail the qualification test  $N - 1$  times, thus ending up in the  $N$ th qualifying minimum.

In the newest version of the software, the latter method is implemented as a separate function. It finds the minimum of the specified order, but, by default, without finally qualifying it, as this might interfere the strict counting of minima. If the  $N$ th *qualifying* minimum is desired, an optional maximum width of the Josephson feature can be specified.

	<b>Improving Band 9 Sensitivity by Advanced Tuning Algorithms — Final Study Report</b>	DocID: FEND-40.02.09.00-1944-C Version: C Date: 2020-01-07 Status: Released Page: 32 of 44
-----------------------------------------------------------------------------------	----------------------------------------------------------------------------------------------------	--------------------------------------------------------------------------------------------------------

## 5 Improvement of existing ALMA mixers

Two sets of historical data were studied to give a meaningful answer to the question how many of the installed ALMA Band 9 junctions can potentially be improved, and by how much, by suppressing them in the first minimum instead of the usual second. Since each of these sets does not contain sufficient information to provide a good estimate, both sets were needed and the results combined. In addition, a smaller set of new measurements were performed specifically for this purpose, where we find a clear linear behaviour of the noise temperature on the magnet current. Together this data gives a reasonable estimate of the expected improvement of the entire array.

### 5.1 Analysis of historical ALMA data

During in-lab commissioning and performance testing of the delivered Band 9 junctions (integrated in the CCAs), full Josephson suppression curves (critical current  $I_C$  vs. magnet current  $I_M$ ) were recorded. From these curves, suitable suppression points, usually in the second minimum for reasons of reproducibility and stability of the tuning, were determined and supplied with the delivery, after they were confirmed to yield in-spec performance (noise temperature, power stability, etc.).

We used an earlier version of the automated tuning algorithm (described in the Midterm Review Report[5]) which only looked at the critical current without refinement using the IF power. Since this simple algorithm was not completely stable, it was replaced by the one described in chapter 4 of the current report. The old algorithm has one advantage, though, namely that it does not require active interaction with the mixers, and so it can be applied to the historical data of the delivered mixers. This was done, and for each mixer the resulting

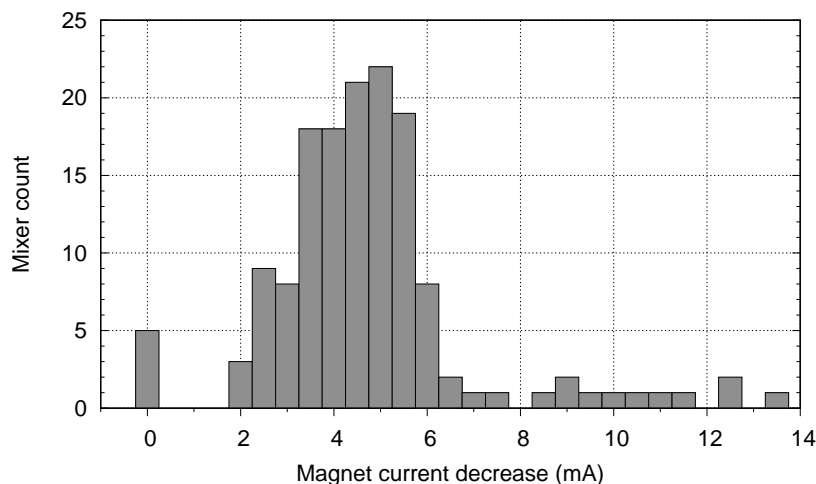


Figure 20: Histogram of the number of delivered Band 9 mixers against the decrease in magnet current when they would be tuned in the first Josephson minimum rather than the minimum supplied as part of the tuning data. For five mixers no lower suppression current is found at all. The bulk (which were qualified in the second minimum) could be tuned 3–6 mA lower, while a few could even come down from the third minimum (>8 mA).

reduction of the magnet current with respect to the supplied setpoint was determined. The results are presented in Fig. 20, which shows a histogram of the number of mixers that could be suppressed in the first minimum, as function of magnet current reduction, in 0.5 mA bins. Three populations can be distinguished: five mixers at 0 mA where no lower minimum was found, the large bulk of 130 mixers (2–8 mA) which were delivered in the second minimum, and above that eleven mixers that were apparently suppressed in the third. The numbers add up to the total of 146 mixers, corresponding to 73 cartridges. Although the final algorithm is more refined, we expect that this still gives a good prediction of the average improvement of all the mixers in the array. Since the first-minimum population cannot be improved much, and the third-minimum one is likely to have problems at low suppression currents, we are left with, conservatively, about 80% of the mixers that could be operated at a significantly lower current.

Now the question is how this reduction in magnet current can be translated into expected reduction of noise temperature.

## 5.2 Analysis of historical CHAMP+ data

Because of the required qualification throughput at the time of Band 9 production, no other minima but the selected one were tested with respect to the noise temperature and other performance parameters. This means that no direct answer, for each mixer individually, can be given on the question of potential noise temperature reduction. However, a few years ago, a batch of about twenty left-over Band 9 AlN-barrier mixers were retested as upgrade candidates for the old  $\text{AlO}_x$  mixers installed in the CHAMP+ low-band array on APEX. This time, noise

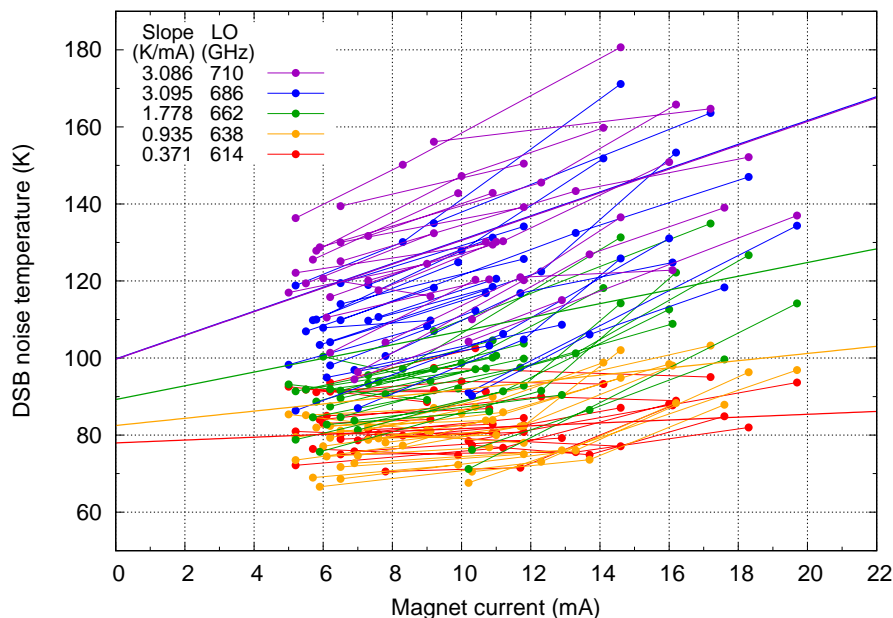


Figure 21: The DSB noise temperature against magnet current of all Band 9 mixers that were retested for CHAMP+ selection for which both first and second minimum data is available. In a few cases also the third minimum was tested, but although they are plotted in this figure, they were not taken into account for the subsequent calculations, for reasons explained in the text.

	<b>Improving Band 9 Sensitivity by Advanced Tuning Algorithms — Final Study Report</b>	DocID: FEND-40.02.09.00-1944-C Version: C Date: 2020-01-07 Status: Released Page: 34 of 44
-----------------------------------------------------------------------------------	----------------------------------------------------------------------------------------------------	--------------------------------------------------------------------------------------------------------

temperatures both in first and second minimum (and sometimes third) were determined. We expect this sample of mixers to be reasonably representative of the ALMA Band 9 population, as they come from the same SIS production batches. Many of them were actually candidates for ALMA delivery but were rejected on grounds of tunability or noise temperature (at the second minimum).

Figure 21 shows the noise temperature of all these retested mixers for which both first and second minima data are available, for five different LO frequencies. Corresponding points are connected by lines. Although there is a large scatter in the data, reasonably clear trends can be seen. At LO frequencies close to the bottom of the band (red and yellow), the lines are almost horizontal, and not much improvement can be obtained. On the other hand, near the top of the band, a pronounced positive slope can be discerned.

Table 2: The average slope in Kelvin per milliampere when going from second to first suppression minimum in the retested CHAMP+ mixers, for five different LO frequencies.

LO freq (GHz)	Slope (K/mA)
614	0.37
638	0.94
662	1.78
686	3.10
710	3.09

To make this more quantitative, the slopes of all connecting line are averaged for each LO frequency, and tabulated in Table 2. For several mixers third minimum data is available as well, and although these are plotted in Fig. 21, they were not included in the average slope calculation for two reasons: the third minimum data are in most cases from different cooldowns, and secondly we are mostly interested in the  $T_N$  reduction going from the second to the first minimum for the bulk of the mixers fall in that category (and the behaviour could easily be non-linear over longer intervals as well). Lines with the averaged slopes are co-plotted in Fig. 21, with arbitrary vertical offsets to locate them close to the data sets they correspond to. Apart from the clear increase in slope with LO frequency, another remarkable feature is that the slope between the highest two LO frequencies (686 and 710 GHz) hardly changes anymore (the blue and purple lines are virtually on top of each other).

It should be stressed that the slopes derived from these historical data differ quite a bit from the ones resulting from the new measurements described in the next section. The discrepancy will be discussed there.

### 5.3 Magnetic field dependence of the noise temperature

While testing the new tuning algorithms, a potentially very important observation was re-established, in the sense that the effect has been seen before, but never systematically investigated for Band 9 junctions. It turns out that the obtainable noise temperature is actually not dependent on the order or depth of the minimum, but simply on the magnitude of the applied magnetic field. This actually inspired us to use the width of the Josephson feature (to ensure that there is a wide enough bias region) rather than its intensity as the main optimization goal.

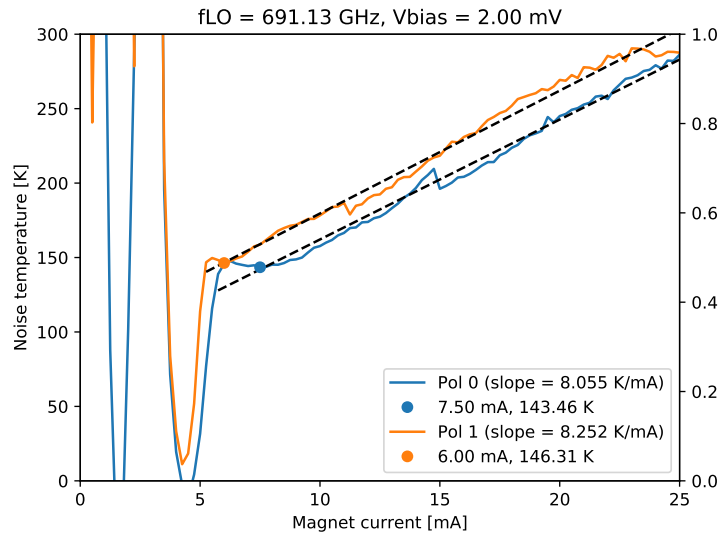


Figure 22: Example of the noise temperature versus magnet current for two different mixers. As soon as the Josephson region shrinks so far that the bias point lies outside of it, we observe a simple straight relationship. The circles denote optimum values for the magnet current.

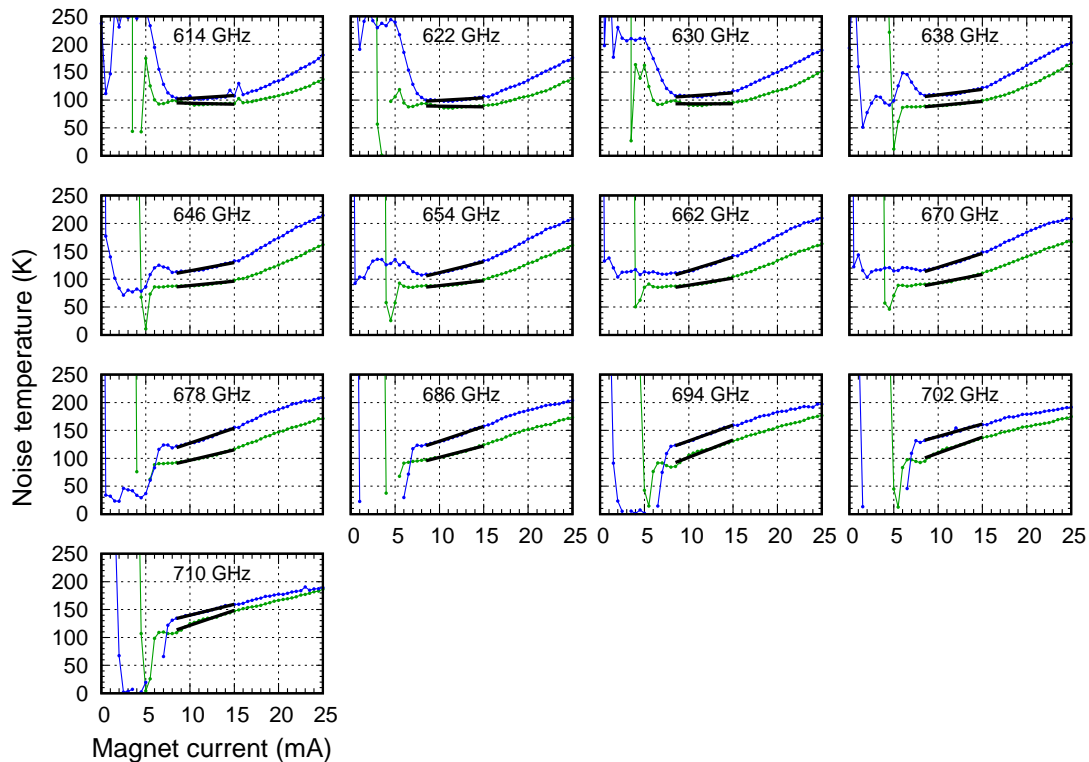


Figure 23: The noise temperature as function of the magnet current for two typical well-behaved mixers, for a series of LO frequencies. The thick black lines represent the (least-square) fits over the relevant regions (currents typical for the first and second minima).

Figure 22 shows an early example of the noise temperature determined at a fixed bias voltage of 2 mV, as a function of magnet current. At some point ( $\approx 5$  mA in this case), the Josephson region shrinks so far in width that the bias point lies outside of it. From that point onwards, we find a simple straight relationship between noise temperature and magnet current. In the particular case of the two tested mixers, we find a slope with a coefficient of about 8 K/mA.

In the Midterm Review Report [5], section 3.4, we described potential procedures that could lead to the best possible suppression, but at the cost of having to tune the Josephson suppression interactively for each LO frequency. Although a small improvement over the procedure described in chapter 4 might still be gained, it was decided after discussion with ESO and ALMA people that this would not be practical in real operations. Instead, we performed a series of new measurements specifically for the purpose of investigating the systematics of the noise temperature vs. magnet current dependency, and therefore its predictive capacity.

Another issue to solve was the discrepancy noted above, between the magnet current dependency found in the early measurement (Fig. 22,  $\approx 8$  K/mA) and the historical CHAMP+ data (section 5.2, 0–3.1 K/mA depending on LO frequency).

The new measurements confirm that there is indeed a strong dependence on the LO frequency, in addition to a strong non-linearity that is most pronounced at low LO frequencies. Fig. 23 shows an overview of a sample of  $T_N$  vs.  $I_M$  curves, where the late upturn is clearly visible up to, say, 670 GHz LO, while at 686 GHz and above the relationship becomes pretty straight.

To determine the potential gain in noise temperature, we made linear fits to these curves (straight black lines), which were confined to the region of the first to the second minimum (as in the case of the CHAMP+ data). The slopes found this way are plotted for all acceptable retested mixers in Fig. 24. As can be seen, the overall behaviour is now much closer to the CHAMP+ data, although there is still a scaling difference. At the same time the spread between mixers at most LO frequencies is about a factor of two or even more. From this we

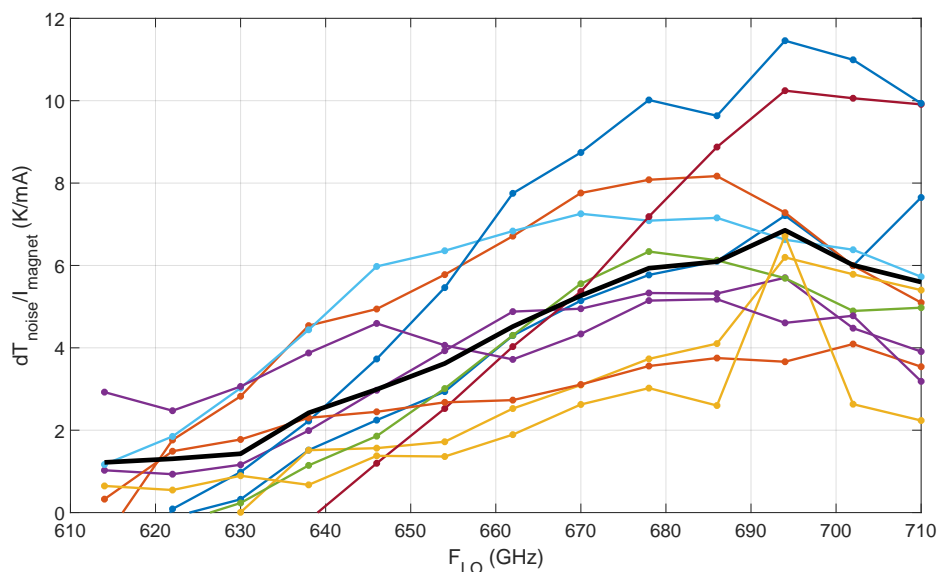


Figure 24: The slopes extracted from the  $T_N$  vs.  $I_m$  curves, as in Fig. 23, for all retested mixers that showed acceptable behaviour (*i.e.*, mixers that would be candidates for qualification in the main array). The thick black line is the average of these data.

	<b>Improving Band 9 Sensitivity by Advanced Tuning Algorithms — Final Study Report</b>	DocID: FEND-40.02.09.00-1944-C Version: C Date: 2020-01-07 Status: Released Page: 37 of 44
-----------------------------------------------------------------------------------	----------------------------------------------------------------------------------------------------	--------------------------------------------------------------------------------------------------------

Table 3: The average slope in Kelvin per milliampere as extracted from the new series of measurement.

LO freq (GHz)	Slope (K/mA)
614	1.22
622	1.31
630	1.43
638	2.42
646	2.99
654	3.62
662	4.52
670	5.27
678	5.93
686	6.09
694	6.85
702	6.01
710	5.60

conclude that the earlier found values (8 K/mA and 3.1 K/mA) are probably accidental outliers within the natural spread. An additional factor may be that the data figure 22 was recorded with constant LO power, while in the measurements described here, the SIS pumping current was kept constant by adjusting the LO power at each magnet current, possibly causing the slopes obtained in both ways not to be completely comparable.

The slopes, averaged over the set of retested mixers are tabulated in table 3. In a few cases where obviously spurious fits were found (*e.g.*, strong negative slopes due to glitches in the suppression), these were excluded from the averages. With the results in this table, we can estimate the improvement in noise temperature of the operational mixers in ALMA.

#### 5.4 Synthesis — prospect of improved ALMA Band 9 performance

Now that we have the statistics of the potential magnet current reduction and the average noise temperature vs. magnet current slopes, we can combine these results. This is illustrated in Fig. 25, which reproduces the histogram of Fig. 20, but now with additional horizontal axes corresponding to the  $T_N$  reduction for LO frequencies at the bottom, middle and top of the band.

Especially at the high end (which is of course particularly interesting because of the presence of the CO(6–5) line at 691 GHz) a reduction of, say, 20 to 30 K with a peak around 26 K could be reached.

Of course, the reductions shown are only potential. What still has to be established is how the mixers behave at these lower suppression points. Especially the gain stability and the compression point should be determined. This has been done on the same selection of junctions in the lab and is the subject of the following sections.

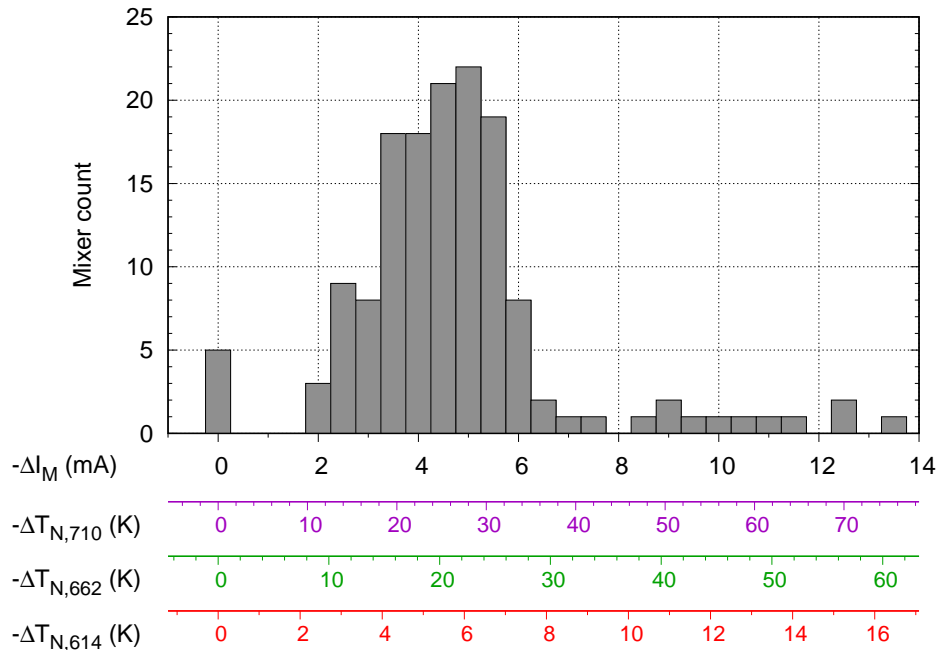


Figure 25: The same histogram as shown in Fig. 20 ( $-\Delta I_M$  is the decrease in magnet current), but now with three additional horizontal scales giving a indications of the corresponding average decrease in noise temperature ( $-\Delta T_{N,LO}$ ), for three LO frequencies, based on the  $T_N$  vs.  $I_M$  calibration obtained from the retested mixer data.

## 5.5 Influence of suppression on other performance parameters

Up to here, the focus of the optimizations has almost exclusively been on the noise temperature. While this *is* the most important parameter determining the efficiency of a receiver, it is certainly not the only one. Several secondary, but still crucial performance parameters should be investigated:

- Amplitude/gain stability, especially when the bias point is chosen closer to the Josephson region;
- Gain compression, which is, among other things, related to the voltage swing over the junction and may therefore become more pronounced when the Josephson regions comes closer to the operating point.

The impact of operating mixers at low magnetic field and closer to the Josephson region these quantities were investigated during the measurement campaign discussed in section 5.3.

### 5.5.1 Stability

The stability of the mixers was tested in the standard way, by determining the Allan variance. Typical results for two different mixers are shown in Fig. 26. In the absence of a magnet current (blue curves) the stability is obviously out of spec, and also the next higher current (4 mA) is clearly not enough for the mixer in the top panel. The latter current is indeed clearly in the Josephson region. As soon as the current passes the first minimum (about 8 mA), there seem to be no issues with the stability anymore (and actually no further improvement). This pattern

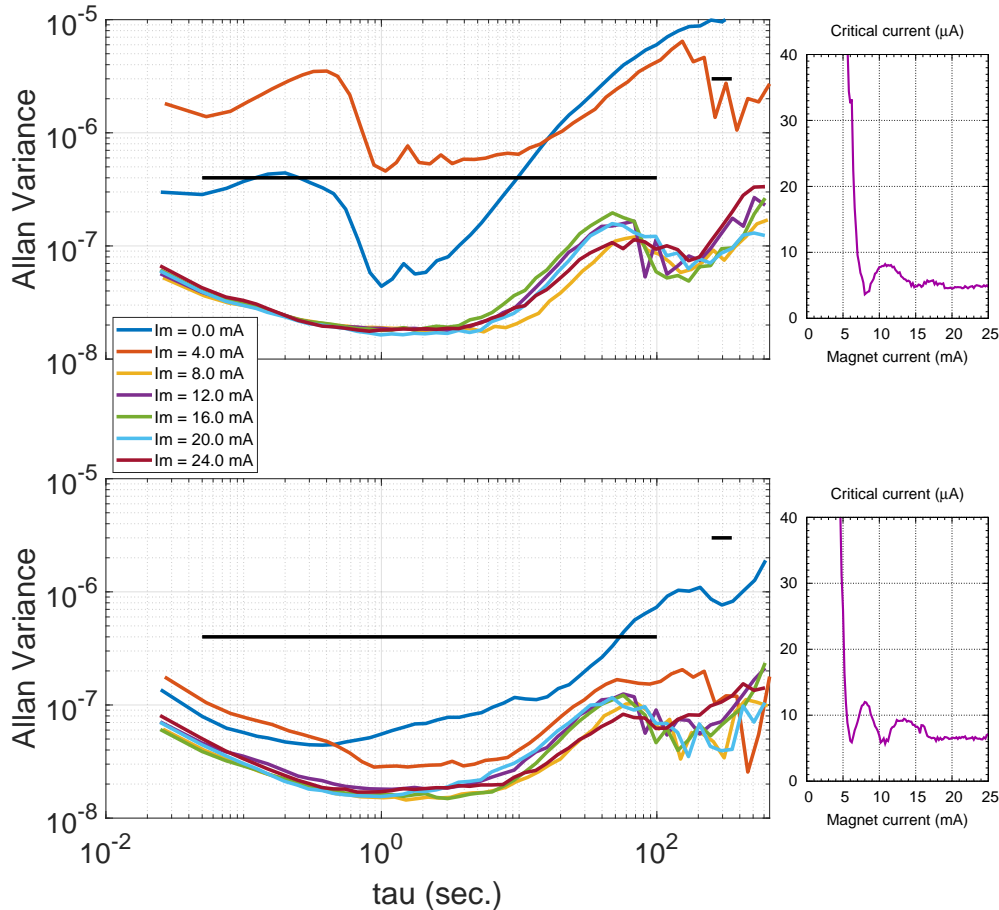


Figure 26: Amplitude stability (expressed as Allan variance) of two mixers for different suppression currents. As long as the current is comparable or larger than the first minimum, the stability is within ALMA specifications (indicated with the horizontal bars). On the right, the corresponding critical currents as function of magnet current are shown.

is quite repeatable for all re-tested mixers. We conclude that because of rapid deterioration of the stability, there is no sense in searching below the first minimum. At the same time, it is also highly likely that a significant number of mixers *can* be operated at the low magnet current associated with the first minimum. It is probably mandatory to verify the stability of all operational mixers at least once after finding the lower suppression points.

### 5.5.2 Gain compression

Two typical results of the measurements of the second critical performance parameter, the gain compression, are shown in Fig. 27. Here, rather similar behaviour is seen: as soon as the magnet current is close to or above the first minimum, the compression is within specifications. Contrary to the stability plots, a further improvement is observed with increasing magnet current. Still, in view of the gain in noise temperature, it would be advisable to keep the current as low as possible. Only of very high dynamic range is needed (*e.g.*, for solar observations), it might be advantageous to go to higher suppression currents. Concludingly, also here we

can say that the first critical current minimum is a good lower limit for the practically usable magnet current. Although the noise temperature could possibly be marginally lower below this point, issues with stability and gain compression crop up pretty soon. To ensure good overall mixer performance, keeping the first minimum, which is clearly recognisable, as lower limit seems the most sensible thing to do.

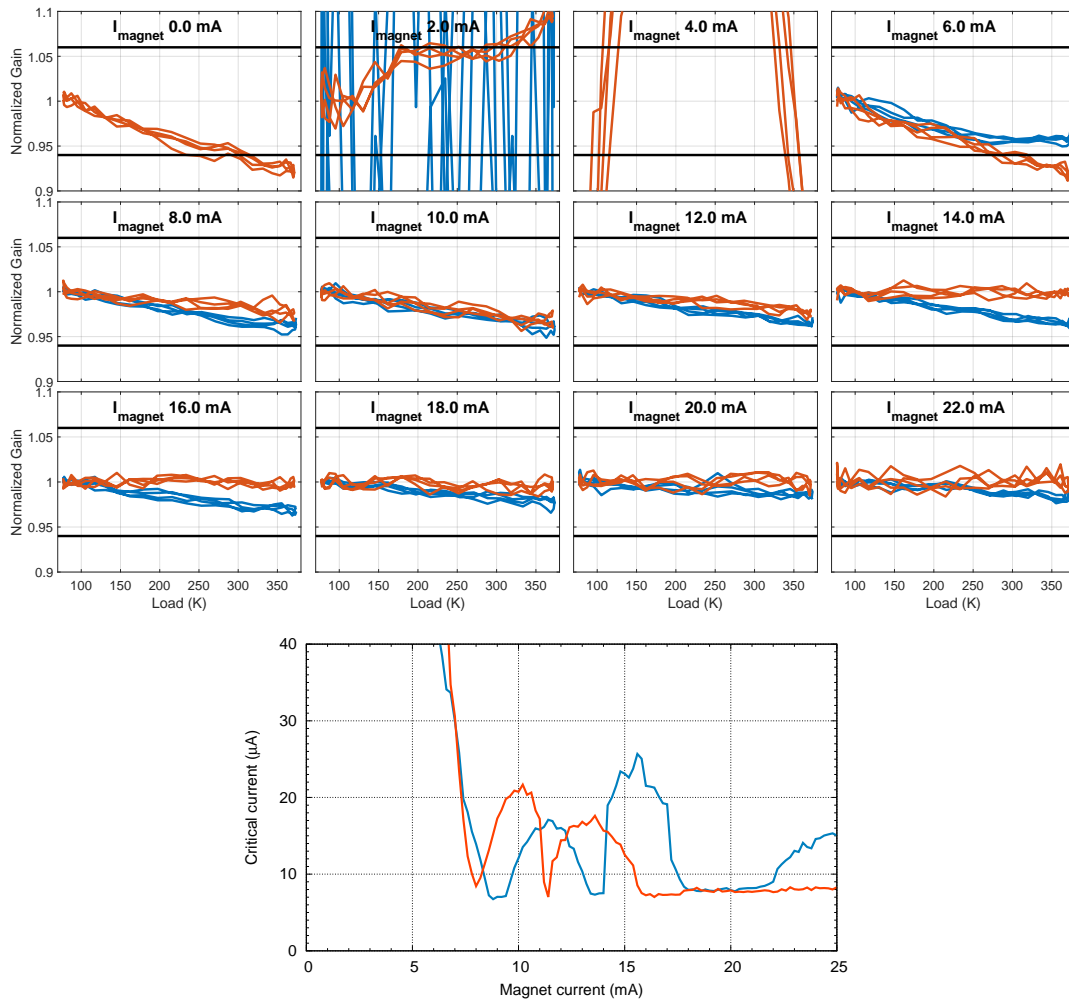


Figure 27: Top: normalized gain curves for two mixers at different magnet currents. The horizontal black lines indicate the maximum deviation allowed by the ALMA gain compression specification. As soon as the magnet current is around the first minimum ( $\approx 8$  mA), the compression is in spec. Below: the corresponding critical currents as function of magnet current.

### 5.5.3 Frequency dependence of the Josephson minima

One final question is whether the optimal suppression points (which we consider for the moment to coincide with Josephson minima) are LO frequency independent. The new mixer measurements seem to confirm this. In each of the mixers, we find that magnet currents for optimum suppression is independent of LO frequency. This is illustrated in Figure 28, which shows maps of the IF power as function of both bias voltage and magnet current, for a series

of LO frequencies In all cases, the minima, marked with horizontal dashed lines occur at the same magnet currents.

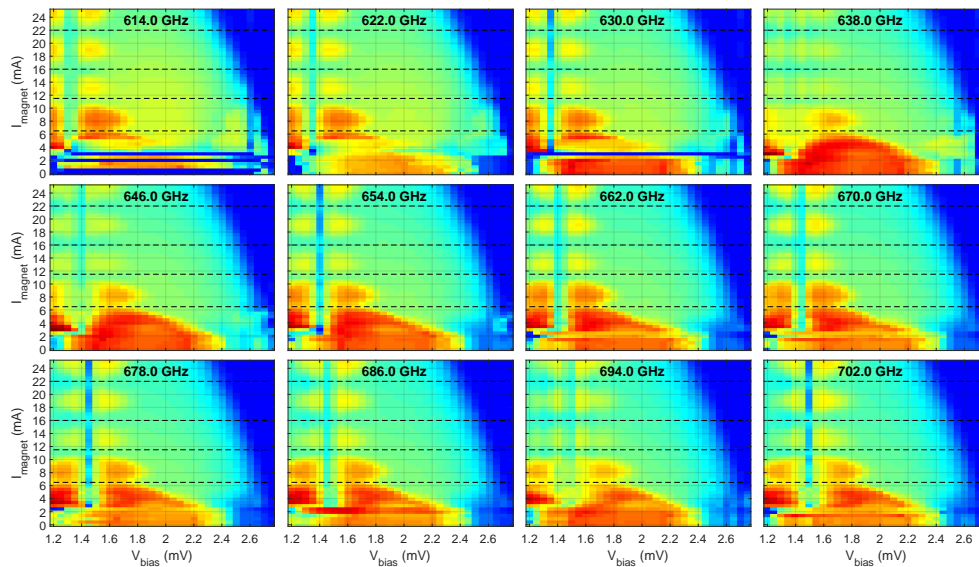


Figure 28: Maps of IF Power vs. magnet current and bias voltage showing the suppression of the Josephson peak, for twelve LO frequencies spread over the entire band. This shows that the magnet currents for optimum suppression (horizontal dashed lines) are independent of the LO frequency.

 <p data-bbox="256 264 394 331">NOVA Sub-mm Instrumentation Group</p>	<p data-bbox="405 136 767 257"><b>Improving Band 9 Sensitivity by Advanced Tuning Algorithms — Final Study Report</b></p>	<p data-bbox="767 136 1327 293">DocID: FEND-40.02.09.00-1944-C Version: C Date: 2020-01-07 Status: Released Page: 42 of 44</p>
----------------------------------------------------------------------------------------------------------------------------------------------------------------	---------------------------------------------------------------------------------------------------------------------------------------	------------------------------------------------------------------------------------------------------------------------------------------------

## 6 Conclusion and outlook

### 6.1 Conclusions

Concludingly we can state that, as outcome of this study (cf. section 1.3),

- We described the issues of automatic tuning, especially those of Josephson suppression;
- We developed a new software framework, based on the ubiquitous programming language Python, which implements a superset of the original *Rodrigo* system used at NOVA for qualification of the Band 9 and Band 5 receiver cartridges;
- We developed an automatic Josephson tuning algorithm operating in three broad steps: initial minimization of the critical current, subsequent refining based on the integrated power of the Josephson feature, and finally qualification based on the width of the Josephson feature;
- We tested the algorithm on eleven left-over Band 9 mixers (several of which were of sub-standard quality) and found it to be robust for this population; apart from finding lower-noise operating points for the Band 9 mixers, we expect this to save a significant amount of operator time;
- We established that a found suppression point for a particular mixer can be used at all LO frequencies throughout the band;
- We established that, in the tested mixers, both the gain compression and amplitude stability specifications are met as soon as the suppression field is at or past the first minimum;
- Finally, applying a simplified (non-interactive) version of the algorithm to the archived data of all delivered Band 9 mixers, we estimate that a large majority of mixers ( $\approx 80\%$ ) can be improved by 15–30 K in noise temperature for the top part of the band, by 10–25 K in the middle, and by a modest 4–7 K at the bottom of the band.

### 6.2 Outlook

The obvious follow-up of this study is the implementation and evaluation of the found algorithms at the ALMA observatory. We propose to do this in two steps: first in the engineering software used at the OSF, and subsequently in the operational front-end control software. This task is clearly set for the software engineers at ALMA, but of course we are highly motivated to assist or collaborate in this effort.

Another interesting question is the applicability of the algorithm to other bands. It is our experience that at lower frequencies (Band 5, in case), the magnetic field is much less critical and typically can be set to a fixed value for all operations; bands up to about 370 GHz are nowadays even suppressed by permanent magnets by some groups. On the higher-frequency side, we very recently applied the tuning algorithm to one of our Band 10 (790–950 GHz) mixers. It was able, almost without modification, to find a correct suppression point. From this, we gather that upwards of ALMA’s Band 6 or 7, benefits similar to the ones we see in Band 9, in terms of operator time and adaptability to changing front-end conditions may be expected. The gain in sensitivity that can be obtained by reliably tuning to lower suppression field is another matter. In the first place, we do not know at the moment to which minima the other ALMA bands are routinely tuned. Secondly, there are a couple of physical arguments why the reduction of magnetic field is so effective in the upper half of the Band 9 mixers, having to do with the gap frequency of niobium (which is about halfway the band) and the

 <p>NOVA Sub-mm Instrumentation Group</p>	<b>Improving Band 9 Sensitivity by Advanced Tuning Algorithms — Final Study Report</b>	DocID: FEND-40.02.09.00-1944-C Version: C Date: 2020-01-07 Status: Released Page: 43 of 44
------------------------------------------------------------------------------------------------------------------------------------	----------------------------------------------------------------------------------------------------	--------------------------------------------------------------------------------------------------------

proximity effect present in the Band 9 junctions. In both lower and higher bands, these effects are expected to be much less pronounced, reducing the expected sensitivity increase to a few percent, as in the bottom end of Band 9. Still, if this can be obtained “for free” by applying careful tuning, it is still a worthwhile benefit.

 <p>NOVA Sub-mm Instrumentation Group</p>	<p><b>Improving Band 9 Sensitivity by Advanced Tuning Algorithms — Final Study Report</b></p>	<p>DocID: FEND-40.02.09.00-1944-C Version: C Date: 2020-01-07 Status: Released Page: 44 of 44</p>
------------------------------------------------------------------------------------------------------------------------------------	-----------------------------------------------------------------------------------------------------------	-------------------------------------------------------------------------------------------------------------------

## 7 References

- [1] Hesper, R., Barkhof, J., Baryshev, A.M. and Boland, W., *Improving Band 9 Sensitivity by Advanced Tuning Algorithms; Scientific – Technical – Management Proposal*, NOVA-ATA-0001-1.2 (2016)
- [2] Alberto D. Bolatto et al., *A road map for developing — ALMA ASAC recommendations for ALMA 2030*
- [3] Alberto D. Bolatto et al., *Pathways to developing ALMA — ALMA development working group report*
- [4] Baryshev, A.M., Hesper, R., Mena, F.P. et al., *The ALMA Band 9 receiver — Design, construction, characterization, and first light*, A&A 577, A129 (2015)
- [5] R. Hesper, T. Vos and J. Barkhof, *Improving Band 9 Sensitivity by Advanced Tuning Algorithms — Midterm Review Report*, NOVA document NOVA-ATA-0002-B (2019)
- [6] T. Vos, *Introducing Novasoft: a new and improved software framework for operating ALMA receivers — Internship report*, document NOVA-ATA-0003-A (2018)
- [7] T. Vos, *An Advanced Tuning Algorithm for Suppressing Josephson Currents in Band 9 ALMA Receivers — Master’s thesis*, document NOVA-ATA-0004-A (2019)
- [8] Barkhof, J., Jackson, B.D., Baryshev, A.M. and Hesper, R., *ALMA Band 9 Cartridge Automated Test System*, Proceedings of the Twentieth International Symposium on Space Terahertz Technology, 246-250 (2009)